Table 5. Histological findings and IL28 genotypes.

SNP	Allele (1/2)	Genotype			p value[a]	OR
		11	12	22		(95% CI)[b]
rs8099917	T/G					
	Fibrosis					
	F0–1	3	38	79	0.036	1.66
	F2–4	5	53	186		(1.03–2.69)
	Activity					
	A0–1	2	35	68	0.025	1.75
	A2–3	6	56	199		(1.07–2.86)

[a] p value by χ^2 test for the minor allele dominant model.
[b] Odds ratio for the minor allele in a dominant model.

(OR = 1.75; $p = 0.025$). Similarly, fibrosis was more severe in patients homozygous for IL28 major alleles (OR = 1.66; $p = 0.036$). We also performed analysis of the association of IL28 alleles and histological findings after adjusting for other factors that might influence the activity and fibrosis of the liver, such as age, gender, and alcoholic consumption. The IL28 allele was associated with F and A factors independently with adjustment for these predictive factors related to severity of liver fibrosis and inflammation (data not shown).

Relationship between histological activity, the IL28 allele, and gamma-GTP

As we described above, histological activity is more active in patients homozygous for IL28 major alleles. However, it seems contradictory that IL28 major allele homozygosity was associated with low levels of gamma-GTP, but severe activity was associated with high gamma-GTP. As shown in Fig. 2, however, when we compare the allele and activity the frequency of patients with higher activity (A2 and A3) were statistically more frequent in patients homozygous for major alleles (Fig. 2 and Table 5). When we compare gamma-GTP levels of A2 and A3 patients between patients homozygous for major alleles against the others, the levels were significantly lower in the major allele homozygous patients (Fig. 2). A0 and A1 patients showed similar results (Fig. 2). gamma-GTP levels are also significantly higher in patients with higher activities (A2 and A3) than in patients with lower activities (A0 and A1) (Fig. 2).

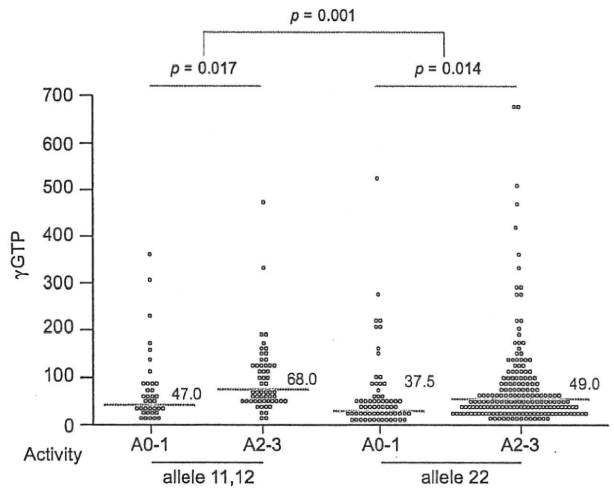

Fig. 2. Relationship between gamma-GTP levels, histological activity and IL28 genotype. gamma-GTP levels are plotted according to IL28 alleles, and histological activity. Horizontal bars represent the median. Mann–Whitney U-test was used to compare gamma-GTP levels.

Discussion

Polymorphism at the IL28 locus has been reported to be associated with the effectiveness of interferon and ribavirin combination therapy [15–17]. We have also found that the polymorphism is associated with the effect of interferon monotherapy on genotype 1b infected patients as well as genotype 2a infection in Japanese as well as Taiwanese patients (Chayama K, personal communication). The polymorphism has also been reported to be associated with spontaneous eradication of the hepatitis C virus [19]. As levels of IL28 gene transcripts have been reported to be higher in patients homozygous for the interferon response allele [16,17], we hypothesized that the polymorphism is also associated with inflammation and progression of chronic hepatitis. As expected, there were significant associations between IL28 genotypes and histological inflammatory activity as well as the degree of fibrosis in chronically HCV infected patients (Table 5). It seems reasonable that the inflammation is stronger in patients with elevated IL28 production because this molecule induces expression of interferon stimulated genes, including some inflammatory cytokines. As the polymorphism is associated with the effect of interferon therapy, the interferon therapy performed before biopsy might alter the results. In fact, a part of patients in this study were treated with peg-interferon and ribavirin combination therapy and the treatment outcome was associated with IL28 genotypes and core amino acid substitutions (data not shown). However, when we analyzed the relation between the IL28 allele and histological findings or core amino acid substitutions in only treatment-naïve patients, the results were unchanged, suggesting that the results obtained in this study are applicable without regard to history of interferon therapy.

Interestingly, the IL28 genotype was also associated with gamma-GTP levels and core amino acid substitutions, both of which are known to be predictive of response to interferon and ribavirin combination therapy [7,8,24]. The levels of liver enzymes such as ALT, AST, and gamma-GTP are usually higher in patients with high inflammatory activity. However, we observed that the levels were actually lower in patients with the favorable allele at the IL28 locus (the major allele in the Japanese population) (Figs. 1A and 2). A lower level of gamma-GTP has been reported to be associated with positive response to combination therapy. Further studies are needed to clarify the mechanism underlying the relation between gamma-GTP levels and therapy effectiveness. It would also be interesting to study the relationship between the IL28 allele and steatosis in the liver because gamma-GTP tends to be elevated in patients with steatosis, and steatosis caused by HCV core protein has been reported [25].

Similarly, viral wild type core amino acids 70 and 91 (i.e., core 70R and 91L), which were already known to be associated with positive response to combination therapy [7,8], were also found to be associated with the favorable human IL28 alleles (Table 3). If viruses with wild type core amino acids 70 and 91 are more

susceptible to interferon therapy, such strains should be less frequent in patients with higher cytokine levels. Viruses with wild type core 70 and 91 amino acids must therefore have some survival advantage in order to replicate in cells in which the level of IL28 production is high. Searching for a target molecule in the signaling cascade from sensing of the virus to production of IL28 might help resolve this question.

We also observed an association between high gamma-GTP levels and core amino acid 70 and 91 substitutions (Fig. 1C), although in multivariate analysis only IL28 genotype, liver fibrosis, sex, and alcohol consumption were significant predictors of gamma-GTP. It seems likely that these factors mutually interact in the presence of the virus and cytokines. Understanding these relationships will reveal the mechanism underlying the effective response to combination therapy and may suggest new strategies to cope with the hepatitis C virus.

Financial disclosure

The authors who have taken part in this study declare that they do not have anything to disclose regarding funding or conflict of interest with respect to this manuscript.

Acknowledgments

The authors thank Rie Akiyama, Yoshie Yoshida, Kazuyo Hattori, Mariko Shiota, Hiromi Ishino, Yasufumi Hayashida, and Takako Yokogi for excellent technical assistance, and Junko Sakamiya, Aya Furukawa, Mika Tsuzuno, Sakura Akamatus, Sanae Furuya, and other secretary members for their secretarial assistance. Part of this work was carried out at the Analysis Center of Life Science, Hiroshima University. This work was supported in part by Grants-in-Aid for scientific research and development from the Ministry of Health, Labor, and Welfare and Ministry of Education Culture Sports Science and Technology, Government of Japan.

References

[1] Barrera JM, Bruguera M, Ercilla MG, Gil C, Celis R, Gil MP, et al. Persistent hepatitis C viremia after acute self-limiting posttransfusion hepatitis C. Hepatology 1995;21:639–644.
[2] Hadziyannis SJ, Sette Jr H, Morgan TR, Balan V, Diago M, Marcellin P, et al. Peginterferon-alpha2a and ribavirin combination therapy in chronic hepatitis C: a randomized study of treatment duration and ribavirin dose. Ann Intern Med 2004;140:346–355.
[3] Manns MP, McHutchison JG, Gordon SC, Rustgi VK, Shiffman M, Reindollar R, et al. Peginterferon alfa-2b plus ribavirin compared with interferon alfa-2b plus ribavirin for initial treatment of chronic hepatitis C: a randomised trial. Lancet 2001;358:958–965.
[4] Jensen DM, Marcellin P, Freilich B, Andreone P, Di Bisceglie A, Brandao-Mello CE, et al. Re-treatment of patients with chronic hepatitis C who do not respond to peginterferon-alpha2b: a randomized trial. Ann Intern Med 2009;150:528–540.
[5] Enomoto N, Sakuma I, Asahina Y, Kurosaki M, Murakami T, Yamamoto C, et al. Mutations in the nonstructural protein 5A gene and response to interferon in patients with chronic hepatitis C virus 1b infection. N Engl J Med 1996;334:77–81.
[6] Enomoto N, Sakuma I, Asahina Y, Kurosaki M, Murakami T, Yamamoto C, et al. Comparison of full-length sequences of interferon-sensitive and resistant hepatitis C virus 1b. Sensitivity to interferon is conferred by amino acid substitutions in the NS5A region. J Clin Invest 1995;96:224–230.
[7] Akuta N, Suzuki F, Kawamura Y, Yatsuji H, Sezaki H, Suzuki Y, et al. Predictive factors of early and sustained responses to peginterferon plus ribavirin combination therapy in Japanese patients infected with hepatitis C virus genotype 1b: amino acid substitutions in the core region and low-density lipoprotein cholesterol levels. J Hepatol 2007;46:403–410.
[8] Akuta N, Suzuki F, Sezaki H, Suzuki Y, Hosaka T, Someya T, et al. Predictive factors of virological non-response to interferon-ribavirin combination therapy for patients infected with hepatitis C virus of genotype 1b and high viral load. J Med Virol 2006;78:83–90.
[9] Welzel TM, Morgan TR, Bonkovsky HL, Naishadham D, Pfeiffer RM, Wright EC, et al. Variants in interferon-alpha pathway genes and response to pegylated interferon-Alpha2a plus ribavirin for treatment of chronic hepatitis C virus infection in the hepatitis C antiviral long-term treatment against cirrhosis trial. Hepatology 2009;49:1847–1858.
[10] Hijikata M, Ohta Y, Mishiro S. Identification of a single nucleotide polymorphism in the MxA gene promoter (G/T at nt −88) correlated with the response of hepatitis C patients to interferon. Intervirology 2000;43:124–127.
[11] Knapp S, Yee LJ, Frodsham AJ, Hennig BJ, Hellier S, Zhang L, et al. Polymorphisms in interferon-induced genes and the outcome of hepatitis C virus infection: roles of MxA, OAS-1 and PKR. Genes Immun 2003;4:411–419.
[12] Matsuyama N, Mishiro S, Sugimoto M, Furuichi Y, Hashimoto M, Hijikata M, et al. The dinucleotide microsatellite polymorphism of the IFNAR1 gene promoter correlates with responsiveness of hepatitis C patients to interferon. Hepatol Res 2003;25:221–225.
[13] Naito M, Matsui A, Inao M, Nagoshi S, Nagano M, Ito N, et al. SNPs in the promoter region of the osteopontin gene as a marker predicting the efficacy of interferon-based therapies in patients with chronic hepatitis C. J Gastroenterol 2005;40:381–388.
[14] Tsukada H, Ochi H, Maekawa T, Abe H, Fujimoto Y, Tsuge M, et al. A polymorphism in MAPKAPK3 affects response to interferon therapy for chronic hepatitis C. Gastroenterology 2009;136:1796–1805, e1796.
[15] Ge D, Fellay J, Thompson AJ, Simon JS, Shianna KV, Urban TJ, et al. Genetic variation in IL28B predicts hepatitis C treatment-induced viral clearance. Nature 2009;461:399–401.
[16] Suppiah V, Moldovan M, Ahlenstiel G, Berg T, Weltman M, Abate ML, et al. IL28B is associated with response to chronic hepatitis C interferon-alpha and ribavirin therapy. Nat Genet 2009;41:1100–1104.
[17] Tanaka Y, Nishida N, Sugiyama M, Kurosaki M, Matsuura K, Sakamoto N, et al. Genome-wide association of IL28B with response to pegylated interferon-alpha and ribavirin therapy for chronic hepatitis C. Nat Genet 2009;41:1105–1109.
[18] Yoneyama M, Kikuchi M, Natsukawa T, Shinobu N, Imaizumi T, Miyagishi M, et al. The RNA helicase RIG-I has an essential function in double-stranded RNA-induced innate antiviral responses. Nat Immunol 2004;5:730–737.
[19] Thomas DL, Thio CL, Martin MP, Qi Y, Ge D, O'Huigin C, et al. Genetic variation in IL28B and spontaneous clearance of hepatitis C virus. Nature 2009;461:798–801.
[20] Desmet VJ, Gerber M, Hoofnagle JH, Manns M, Scheuer PJ. Classification of chronic hepatitis: diagnosis, grading and staging. Hepatology 1994;19:1513–1520.
[21] Ohnishi Y, Tanaka T, Ozaki K, Yamada R, Suzuki H, Nakamura Y. A high-throughput SNP typing system for genome-wide association studies. J Hum Genet 2001;46:471–477.
[22] Suzuki A, Yamada R, Chang X, Tokuhiro S, Sawada T, Suzuki M, et al. Functional haplotypes of PADI4, encoding citrullinating enzyme peptidylarginine deiminase 4, are associated with rheumatoid arthritis. Nat Genet 2003;34:395–402.
[23] Kato N, Hijikata M, Ootsuyama Y, Nakagawa M, Ohkoshi S, Sugimura T, et al. Molecular cloning of the human hepatitis C virus genome from Japanese patients with non-A, non-B hepatitis. Proc Natl Acad Sci USA 1990;87:9524–9528.
[24] Bergmann JF, Vrolijk JM, van der Schaar P, Vroom B, van Hoek B, van der Sluys Veer A, et al. Gamma-glutamyltransferase and rapid virological response as predictors of successful treatment with experimental or standard peginterferon-alpha-2b in chronic hepatitis C non-responders. Liver Int 2007;27:1217–1225.
[25] Moriya K, Fujie H, Shintani Y, Yotsuyanagi H, Tsutsumi T, Ishibashi K, et al. The core protein of hepatitis C virus induces hepatocellular carcinoma in transgenic mice. Nat Med 1998;4:1065–1067.

Antiviral Therapy 2010 15:177–184 (doi: 10.3851/IMP1508)

Original article

Differential effects of interferon and lamivudine on serum HBV RNA inhibition in patients with chronic hepatitis B

Yi-Wen Huang[1,2], Kazuaki Chayama[3,4], Masataka Tsuge[3,4], Shoichi Takahashi[3,4], Tsuyoshi Hatakeyama[3,4], Hiromi Abe[3,4], Jui-Ting Hu[1,5], Chun-Jen Liu[2,6], Ming-Yang Lai[2,6], Ding-Shinn Chen[2,6], Sien-Sing Yang[1,5], Jia-Horng Kao[2,6,7]**

[1]Liver Unit, Cathay General Hospital Medical Center, Taipei, Taiwan
[2]Division of Gastroenterology, Department of Internal Medicine, National Taiwan University College of Medicine and National Taiwan University Hospital, Taipei, Taiwan
[3]Department of Medicine and Molecular Science, Division of Frontier Medical Science, Programs for Biomedical Research, Graduate School of Biomedical Sciences, Hiroshima University, Hiroshima, Japan
[4]Liver Research Project Center, Hiroshima University, Hiroshima, Japan
[5]Faculty of Medicine, Fu-Jen Catholic University College of Medicine, Taipei, Taiwan
[6]Graduate Institute of Clinical Medicine, National Taiwan University College of Medicine, Taipei, Taiwan
[7]Hepatitis Research Center, National Taiwan University Hospital, Taipei, Taiwan

*Corresponding authors e-mail: kaojh@ntu.edu.tw; jaab@cgh.org.tw

Background: Lamivudine and interferon have been widely used for the treatment of patients with chronic HBV infection. Serum HBV RNA is detected during lamivudine therapy as a consequence of interrupted reverse transcription and because RNA replicative intermediates are unaffected by the drug. In this study, we aimed to determine the detectability of serum HBV RNA during sequential combination therapy of interferon and lamivudine.

Methods: HBV DNA and RNA in serum samples were quantified by reverse transcription of HBV nucleic acid extract and real-time PCR. Samples were analysed every 2 weeks to 3 months from three groups of patients: 10 male patients treated with nucleoside analogue monotherapy for 44–48 weeks (5 with lamivudine and 5 with entecavir), 6 males on sequential interferon and lamivudine combination therapy, and 3 males on lamivudine monotherapy for 20–24 weeks.

Results: HBV RNA was not detectable in any patients before treatment, but became detectable in 15 during antiviral treatment. Among the three groups, pre-treatment HBV DNA (8.1 ±2.4 versus 7.7 ±1.4 versus 5.1 ±0.3 $\log_{10}$ copies/ml; P=0.06), treatment and follow-up durations (45.5 ±2.0 versus 49.7 ±5.6 versus 48.7 ±6.4 weeks; P=0.32) were comparable. HBV RNA was detectable at the end of treatment or follow-up in all patients with monotherapy, but in none of those with sequential combination therapy (100% versus 0%; P<0.001).

Conclusions: Compared with lamivudine therapy with detectable serum HBV RNA in patients with chronic HBV infection, interferon treatment might reduce HBV DNA replication through the inhibition of HBV RNA replicative intermediates, resulting in the loss of serum HBV RNA.

Introduction

Although effective HBV vaccines have been available for more than two decades, HBV infection remains a global health problem. It is estimated that more than 350 million people are chronic carriers of HBV worldwide [1,2]. In the US, 1.2 million individuals have chronic HBV infection [3]. HBV infection causes a wide spectrum of clinical manifestations, ranging from acute or fulminant hepatitis to various forms of chronic liver disease, including inactive carrier state, chronic hepatitis, cirrhosis and even hepatocellular carcinoma [2,4].

HBV is a unique DNA virus that replicates via pre-genomic RNA. There are several key steps in HBV replication. Firstly, in the nucleus of infected hepatocytes, the asymmetric DNA in virions converts to

covalently closed circular DNA (cccDNA); the cccDNA is then transcribed to pre-genomic RNA. Next, the minus strand of viral DNA is synthesized by reverse transcriptase. Finally, there is synthesis of the plus strand to form mature genomic DNA [5]. Both interferon and nucleos(t)ide analogues have been approved for the treatment of chronic hepatitis B (CHB). All of these agents have viral suppression effects, whereas interferon has additional immunomodulatory properties [6]. Lamivudine is the first approved nucleoside analogue for the treatment of CHB; however, it does not affect the integrated HBV DNAs or their transcripts, the RNA replicative intermediates [7]. Thus, lamivudine, as well as other nucleos(t)ide analogues, needs indefinite duration of therapy for continued viral suppression. By contrast, interferon has a finite duration of therapy and a higher rate of hepatitis B surface antigen (HBsAg) seroclearance than nucleos(t)ide analogues [8]. Our study and others showed that serum HBV RNA could be detected during lamivudine therapy, as the consequence of unaffected RNA replicative intermediates as well as interrupted reverse transcription [9,10]. In addition, serum HBV RNA might serve as a predictor of early emergence of viral mutation during lamivudine therapy [10].

Previous clinical trials indicated that simultaneous combination therapy of interferon-α plus lamivudine leads to greater on-treatment viral suppression and higher sustained response rates than lamivudine monotherapy [8]. However, the detectability and patterns of serum HBV RNA in patients receiving sequential combination therapy of interferon and lamivudine compared with those on lamivudine monotherapy remain largely unknown. Thus, we explored the differential effects of interferon and lamivudine on serum HBV RNA inhibition in CHB patients with various treatment regimens.

Methods

Patients

We enrolled 19 CHB patients treated with nucleoside analogue alone or sequential combination therapy of conventional interferon and lamivudine. These patients were divided into three groups on the basis of treatment regimen. Group I consisted of 10 male patients (mean age 44.2 years; range 30–74) treated with nucleoside analogue monotherapy for 44–48 weeks (5 patients with lamivudine and 5 with entecavir). Group II consisted of six male patients (mean age 47.3 years; range 39–56). Five of these patients were treated with lamivudine for 34–52 weeks and then shifted to conventional interferon for 24–36 weeks; there was an overlap of the two drugs for 4–20 weeks. The remaining patient in this group was treated with conventional interferon for 36 weeks and then shifted to lamivudine for 32 weeks; there was an overlap of the two drugs for 12 weeks. Group III consisted of three male patients (mean age 51.3 years; range 41–64) who were treated with lamivudine for 20–24 weeks and then followed for 22–36 weeks. Serum samples from enrolled patients were obtained just before the initiation of therapy and every 2 weeks to 3 months until the end of treatment or follow-up. These samples were stored at -80°C until use. Informed consent was obtained from each patient.

Extraction of HBV nucleic acid and reverse transcription

Extraction of HBV nucleic acid and reverse transcription with subsequent quantification were performed as previously described [10]. Nucleic acid was extracted from 100 μl serum using the SMI TEST EX-R&D kit (Genome Science Laboratories, Tokyo, Japan) and dissolved in 18 μl of ribonuclease-free water. The extract was then divided into two aliquots of equal size, termed solutions I and II. Solution I was mixed with an equivalent amount of water for DNA quantification. Solution II underwent reverse transcription using a random primer (Takara Bio Inc., Shiga, Japan) and M-MLV reverse transcriptase (ReverTra Ace, TOYOBO Co., Osaka, Japan) with subsequent DNA plus cDNA quantification. The steps in reverse transcription were as follows: 25 pM random primer was added and the sample heated to 65°C for 5 min; the sample was then put on ice for 5 min; 5× reverse transcription buffer (4 μl), 10 mM dNTPs (2 μl), 0.1 M dithiothreitol (2 μl), 8 units of ribonuclease inhibitor and 100 units of M-MLV reverse transcriptase were added; the sample was incubated at 30°C for 10 min and 42°C for 60 min; and inactivation was carried out at 99°C for 5 min.

Quantification of HBV DNA and cDNA by real-time PCR

HBV DNA and cDNA quantification were performed as previously described [10]. A 1 μl aliquot of solution I and solution II were each amplified by real-time PCR with an ABI Prism 7300 Sequence Detection System (Applied Biosystems, Foster City, CA, USA) according to the manufacturer's instructions. Amplification was performed in a 25 μl reaction mixture containing SYBR Green PCR Master Mix (Applied Biosystems), 200 nM forward primer (5′-TTTGGGGCATGGACATTGAC-3′, nucleotides 1893–1912), 200 nM reverse primer (5′-GGTGAACAATGGTCCGGAGAC-3′, nucleotides 2029–2049) and 1 μl of solution I or solution II. The steps in real-time PCR were as follows: incubation at 50°C for 2 min, denaturation at 95°C for 10 min, and PCR cycling comprising 40 two-step cycles of 15 s at 95°C and 60 s at 60°C. The lower detection limit of this assay was 10^3 copies/ml. The HBV RNA quantity is obtained by subtracting the quantification result of solution I from solution II (that is, HBV nucleic acid determined by real-time PCR after reverse transcription reaction minus HBV DNA determined by real-time PCR).

Serological assays

Serum hepatitis B e antigen (HBeAg) and levels of antibodies against HBV e antigen (anti-HBe) were tested by chemiluminescent immunoassay (Architect HBeAg and Architect HBeAb, Abbott Japan, Tokyo, Japan).

Statistical analysis

Baseline characteristics including age, gender, serum alanine aminotransferase (ALT) level, HBeAg and HBV DNA level were compared among study groups. Continuous variables were expressed as mean ± SD and evaluated by Student's *t*-test for comparison between two groups and by Kruskal–Wallis test for comparison among three groups. Categorical variables were expressed as frequencies with proportions and compared using Pearson's χ^2 test; Fisher's exact test was applied when at least one cell of the table has an expected frequency <5. All of the tests were two-tailed and a *P*-value <0.05 was considered statistically significant.

Results

Demographic profiles of patients

Baseline characteristics of CHB patients treated with nucleoside analogues and/or conventional interferon are shown in Table 1. There was no significant difference in terms of age, gender ratio, ALT level, HBeAg status or HBV DNA level among the three groups.

Serum HBV RNA levels after nucleoside analogue therapy

The detectability of serum HBV RNA before, after and at the end of nucleoside analogue therapy or follow-up is shown in Table 2. Serum HBV RNA was undetectable in all patients before the initiation of nucleoside analogue therapy; however, it became detectable in 15 patients (79%) after therapy. Of 14 patients treated with lamivudine, serum HBV RNA was detectable in 10 (71%). By contrast, of five patients treated with entecavir, all (100%) had detectable serum HBV RNA. The peak serum HBV RNA level ranged from 4.2 to 7.0 $\log_{10}$ copies/ml in lamivudine-treated patients and from 7.2 to 9.6 $\log_{10}$ copies/ml in entecavir-treated patients.

Serum HBV RNA levels after interferon treatment in patients with prior lamivudine therapy

In patients with detectable serum HBV RNA after nucleoside analogue monotherapy, HBV RNA persisted until the end of therapy (group I; Table 2). Similarly, serum HBV RNA was persistently detectable after short-term lamivudine therapy (group III; Table 2). By contrast, those with sequential lamivudine and interferon therapy experienced undetectable

Table 1. Baseline characteristics of chronic hepatitis B patients treated with nucleoside analogues and/or conventional interferon

Characteristic	Group I[a]	Group II[b]	Group III[c]	*P*-value
Patients (3TC/ETV), *n*	10 (5/5)	6	3	–
Mean age, years ±SD	44.2 ±13.7	47.3 ±6.5	51.3 ±11.7	0.31[d]
Gender (male/female), *n*	10/0	6/0	3/0	1.0[e]
Mean ALT, U/l ±SD	164.4 ±105.5	180.3 ±121.2	154 ±142	0.88[d]
HBeAg, % (+/-)	70 (7/3)	17 (1/5)	66.7 (2/1)	0.13[e]
Mean HBV DNA, $\log_{10}$ copies/ml ±SD	8.1 ±2.4	7.7 ±1.4	5.1 ±0.3	0.06[d]

[a]Group I, lamivudine (3TC) or entecavir (ETV) monotherapy for 44–48 weeks. [b]Group II, sequential 3TC for 34–52 weeks and conventional interferon for 24–36 weeks; there was overlap of the two drugs for 4–20 weeks. [c]Group III, 3TC therapy for 20–24 weeks, then follow-up for 22–36 weeks. [d]Kruskal–Wallis test; [e]Fisher's exact test. ALT, alanine aminotransferase; HBeAg, hepatitis B e antigen.

Table 2. Serum HBV RNA in chronic hepatitis B patients treated with nucleoside analogues and/or conventional interferon

	Group I[a]	Group II[b]	Group III[c]	*P*-value
Patients (3TC/ETV), *n*	10 (5/5)	6	3	–
Detectability before treatment, %	0	0	0	1.0[e]
Detectability after treatment, *n* (%)	8/2 (80.0)	5/1 (83.0)	2/1 (66.7)	1.0[e]
Mean peak level, $\log_{10}$ copies/ml ±SD	7.4 ±1.9	6.1 ±0.9	4.6 ±0.1	0.08[d]
Mean total duration (treatment plus follow-up), weeks ±SD	45.5 ±2.0	49.7 ±5.6	48.7 ±6.4	0.32[d]
Detectability at end of treatment plus follow-up, *n* (%)	8/0 (100)	0/5 (0)	2/0 (100)	<0.001[e]

[a]Group I, lamivudine (3TC) or entecavir (ETV) monotherapy for 44–48 weeks. [b]Group II, sequential 3TC for 34–52 weeks and conventional interferon for 24–36 weeks; there was overlap of the two drugs for 4–20 weeks. [c]Group III, 3TC therapy for 20–24 weeks, then follow-up for 22–36 weeks. [d]Kruskal–Wallis test; [e]Fisher's exact test.

Figure 1. Sequential changes of serum HBV RNA, DNA and ALT levels in patients treated with lamivudine or entecavir monotherapy for 44–48 weeks with detectable serum HBV RNA (group I)

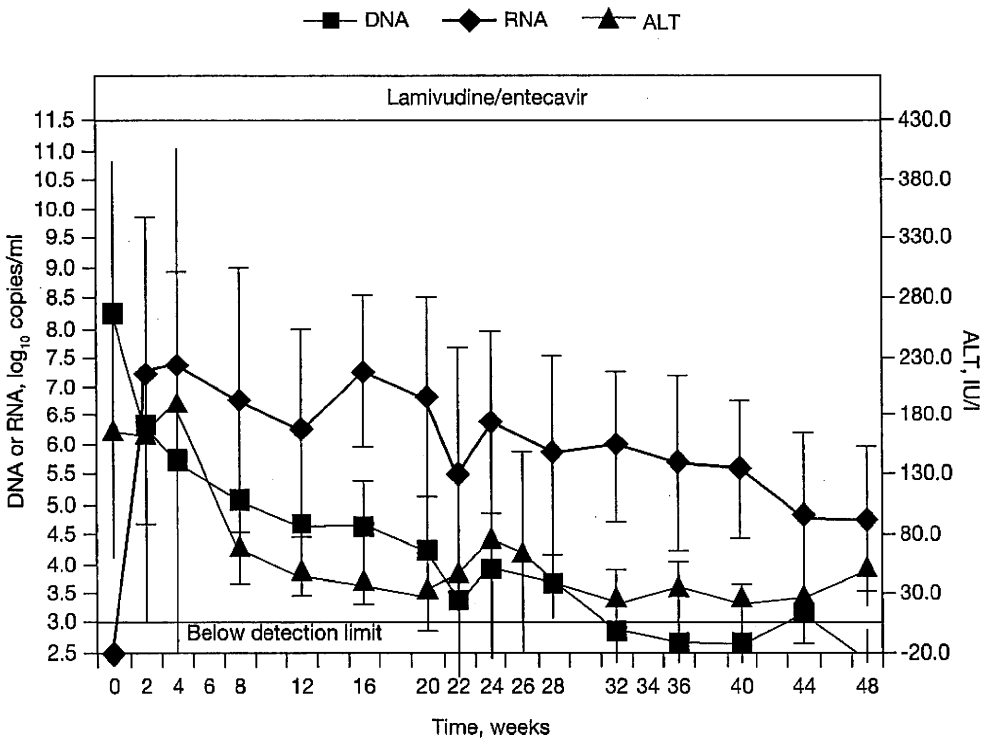

Serum HBV RNA was detectable until the end of treatment. ALT, alanine aminotransferase.

serum HBV RNA at the end of treatment (group II; Table 2).

Sequential changes of serum HBV RNA levels in patients with various treatments

The sequential changes of serum HBV RNA in patients with detectable HBV RNA in group I, II and III are shown in Figure 1, Figure 2 and Figure 3, respectively. As early as 2–4 weeks after starting nucleoside analogue therapy, serum HBV RNA could be detected in 13 patients (87%) and reached the peak level in 11 (73%).

Discussion

The specific presence of serum HBV RNA in patients with CHB infection was confirmed in our previous study using ribonuclease digestion [10]. Ribonuclease treatment reduced the amount of HBV DNA detected by real-time PCR after reverse transcription to about 1% of that originally detected [10]. In this study, detectable serum HBV RNA persisted during nucleoside analogue therapy including lamivudine and entecavir (group I), whereas it was inhibited under sequential lamivudine and interferon therapy (group II). The difference between these two groups is significant even in a small number of patients, demonstrating the substantial HBV RNA inhibitory effect of interferon. The decline in serum HBV RNA level was not simply the result of discontinuation of lamivudine, because serum HBV RNA was persistently detectable even after discontinuation of short-term lamivudine therapy in group III patients. The inhibition of serum HBV RNA was found in patients treated with lamivudine and then shifted to conventional interferon and in those on conventional interferon treatment and shifted to lamivudine. In the latter patients, the inhibition of serum HBV RNA might be due to the delayed therapeutic effect of interferon.

Several previous studies have proven that sequential combination therapy of lamivudine and interferon has a better efficacy than lamivudine monotherapy. For example, sequential lamivudine and interferon therapy increased HBeAg seroconversion rate [11] and had a higher response rate in terms of sustained HBeAg seroconversion, ALT normalization, HBV DNA loss and reduced rates of relapse after stopping therapy [12]. In addition, the initial use of lamivudine before interferon

Figure 2. Sequential changes of serum HBV RNA, DNA and ALT levels in patients treated with lamivudine for 34–52 weeks with detectable serum HBV RNA (group II)

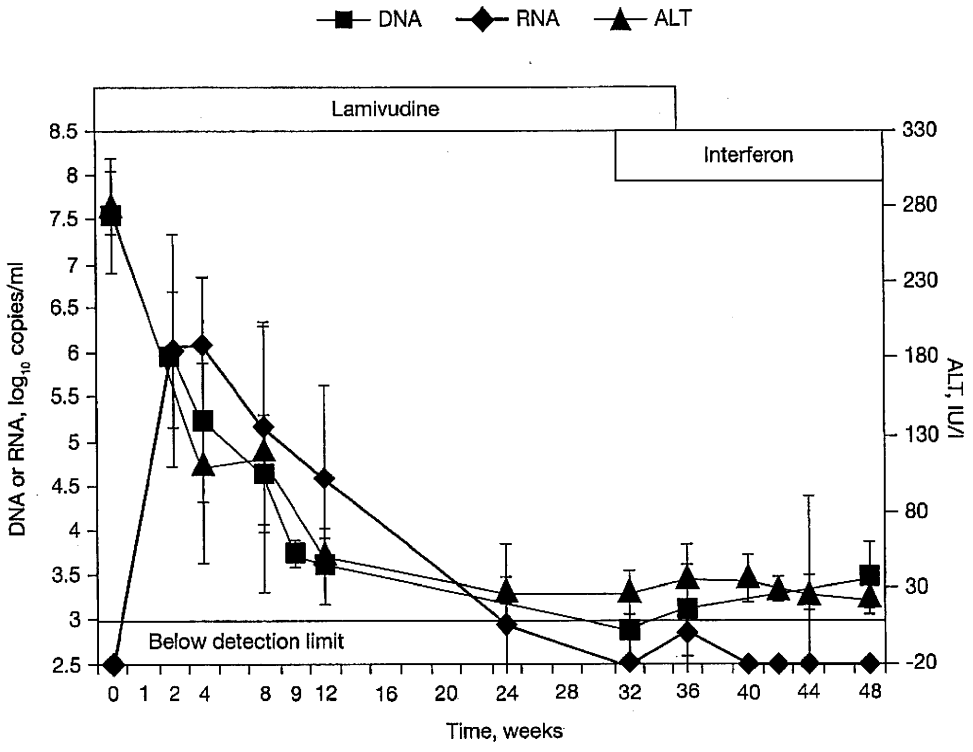

Patients were treated with lamivudine for 34–52 weeks and then shifted to conventional interferon therapy for 24–26 weeks; there was overlap of the two drugs for 4–20 weeks. Serum HBV RNA was undetectable at the end of treatment. ALT, alanine aminotransferase.

led to an improved sustained virological response compared with the use of interferon alone from the start [13]. Nevertheless, the underlying mechanisms of these convincing findings remain unclear and deserve further investigation. In this study, the inhibitory effect of interferon on serum HBV RNA in lamivudine-treated patients might explain why these patients have a higher sustained response rate than those treated with lamivudine monotherapy.

The weak point of this study is the small number of patients in groups II and III. Because this is a pilot study on the differential effects of various treatment regimens on serum HBV RNA, and because the treatment regimens in group II and group III patients are not the current standard of care, we did not intend to include additional patients treated with these regimens. In line with this study, however, our unpublished data on three patients also indicate that *de novo* combination therapy of pegylated interferon plus lamivudine therapy could inhibit serum HBV RNA levels. In these three patients, serum HBV RNA levels started to rise at 12–24 weeks of combination therapy and became undetectable at 48–72 weeks of therapy (YWH, JHK, *et al.*, unpublished data).

Figure 3. Sequential changes of serum HBV RNA, DNA and ALT levels in patients treated with short-term lamivudine for 20–24 weeks with detectable serum HBV RNA (group III)

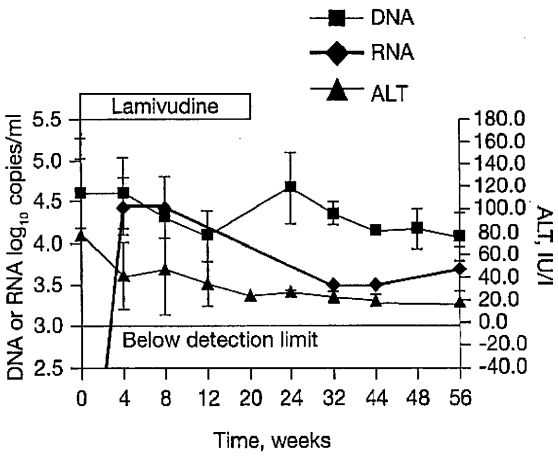

Serum HBV RNA was detectable until the end of follow-up at 44–56 weeks. ALT, alanine aminotransferase.

The presence of serum HBV RNA in patients treated with nucleoside analogues could be explained by *in vitro* data obtained in HBV-transfected HepG2.2.15 cell lines. Doong *et al.* [7] demonstrated that HBV-specific RNAs in cell lysate were not reduced after lamivudine and other nucleoside analogue treatments. Our unpublished data also showed persistent detectable HBV RNA in supernatant from day 4 to 17 of nucleoside analogue treatment when all the cells died (YWH, JHK, *et al.*, unpublished data). Lamivudine and other nucleoside analogues do not affect the integrated HBV DNAs from which HBV RNAs are transcribed [7]. Further studies are needed to evaluate the effect of long-term treatment of nucleoside analogues on serum HBV RNA.

The inhibition of serum HBV RNA by interferon-α might be supported by previous studies on transgenic mice. Intrahepatic HBV replicative intermediates were cleared by a single injection of the interferon-α/β inducer polyinosinic-polycytidylic acid [14]. It was postulated that the mechanism of action of interferon involves the post-transcriptional steps of the HBV life cycle, as the intrahepatic HBV replicative intermediates were cleared while the steady-state content of HBV RNA was unaffected [14]. This same group of researchers further demonstrated that the inhibitory effect of interferon-α/β is at the level of the capsids containing pre-genomic RNA, acting either to accelerate their degradation or to prevent their assembly [15]. Interferon might directly inhibit HBV synthesis or could act through the cellular immune response against HBV-infected hepatocytes [16]. HBV inhibition in immortalized hepatocyte cell lines from HBV transgenic mice by interferon-β and interferon-γ confirms the non-cytolytic inhibition pathway [17]. This inhibition might act through the 2′,5′-oligoadenyl synthetase/RNAse L pathway [18]. Interferon can induce this multienzyme pathway that includes 2′,5′-oligoadenyl synthetase, endoribonuclease RNAse L and 2′,5′-oligoadenyl phosphodiesterase. Among these enzymes, RNAse L theoretically inhibits all viral replication that uses an RNA intermediate step [16]. Furthermore, activation of this ribonuclease has been proposed as the major driver by which interferon inhibits viral replication [18].

In the current study, we performed frequent detection of serum HBV DNA and RNA, in some cases as often as every 2 weeks, to determine the sequential change of serum HBV DNA and RNA during monotherapy or combination therapy. Our data showed that the peak serum HBV RNA level with entecavir treatment was significantly higher than that with lamivudine treatment (8.6 ±1.0 versus 5.6 ±1.0; $P<0.001$). There was also a trend towards higher detectability of serum HBV RNA in patients treated with entecavir in comparison with those treated with lamivudine (100% versus 71%; $P=0.48$). These findings suggest that the serum HBV RNA level might reflect the antiviral potency of nucleoside analogues [19]. Further studies are needed to clarify this interesting and important issue.

Although Rokuhara *et al.* [20] showed that HBV RNA was detectable before lamivudine therapy in serum samples of 24 patients, the detection rate was not specified. Their results of sucrose density gradient fractionation studies indicated that viral particles containing HBV DNA were dominant at the start of treatment, whereas those containing HBV RNA became more prevalent after 1 and 2 months of treatment. They also suggested that under untreated conditions, viral particles containing HBV RNA accounted for only about 1% of total HBV virions. However, these specific particles became the major component under lamivudine treatment [9]. They concluded, therefore, that HBV RNA particles seemed to exist in <1% of the HBV virions among patients without lamivudine treatment [21]. By contrast, the undetectable pre-treatment HBV RNA data in this study was consistent with our previous report, showing that serum HBV RNA levels increased soon after the administration of nucleoside analogues [10]. Furthermore, our data was supported by the *in vitro* data obtained in HBV-transfected HepG2.2.15 cell lines (YWH, JHK, *et al.*, unpublished data), suggesting that HBV RNA was undetectable in the supernatant before nucleoside analogue treatment but became detectable after administration of these agents. In addition, Rokuhara and colleagues [20] reported a more significant decline of the serum HBV DNA level than HBV RNA level during lamivudine therapy, which confirmed our findings.

Serum HBV RNA was persistently detectable even after discontinuation of short-term lamivudine therapy in group III patients. This finding suggested that, although new viral particles containing HBV RNA were no longer produced after discontinuation of lamivudine, the existing viral particles containing HBV RNA during lamivudine administration were not quickly degraded. The study by Rokuhara *et al.* [20] showed a more significant decline in serum HBV DNA than RNA during lamivudine therapy, also confirming our findings on the poor immediate inhibition of serum viral particles containing HBV RNA by nucleoside analogues. Nevertheless, further studies are needed to demonstrate how long the viral particles containing HBV RNA persist in serum.

Following sequential combination therapy of lamivudine and conventional interferon, the serum HBV DNA level declined but was still detectable in all patients until the end of treatment. By contrast, serum HBV RNA was inhibited and undetectable at the end of treatment. The persistent presence of serum HBV DNA was due to the discontinuation of nucleoside analogue treatment and, thus, the lack of

continuous inhibition. The shift to interferon led to the inhibition of serum HBV RNA, but the inhibitory effect of interferon on HBV DNA was not as efficient as that of the nucleoside analogue [8]. Although northern and Southern hybridization data of intracellular RNA and DNA were not available, our study and others have confirmed the possibility of detecting serum HBV RNA. We reported the discrepant measurement of HBV nucleic acid by the transcription-mediated amplification and hybridization protection assay (TMA-HPA) and the Amplicor HBV Monitor test [10]. Because TMA-HPA uses RNA transcription and amplification of transcripts by T7 RNA polymerase [22], we assumed that the discrepancy was a result of the persistence of serum HBV RNA in nucleoside-analogue-treated patients. Zhang *et al.* [9] reported the presence of serum HBV RNA in a patient treated with lamivudine. The study mainly analysed truncated HBV RNA, which was assumed to be transcribed from the integrated HBV genome; the authors showed a marked difference between truncated HBV RNA and HBV DNA. In this study, HBV DNA and HBV nucleic acid were assayed by real-time PCR and real-time reverse transcriptase PCR, and <1 $\log_{10}$ difference was shown; this observation suggests that the effect of truncated serum HBV RNA was minimal. In addition, Rokuhara *et al.* [20] investigated the incorporation of HBV RNA into virus particles using sucrose gradient analyses: HBV RNA made a single peak in one fraction, whereas both HBV DNA and HBV core-related antigen made single peaks at three different time points during lamivudine treatment.

In conclusion, interferon can inhibit serum HBV RNA induced by lamivudine therapy. The persistence of serum HBV RNA as a consequence of unaffected HBV RNA replicative intermediates might lead to indefinite nucleoside analogue therapy. By contrast, the inhibitory effect of interferon on HBV RNA replicative intermediates might potentiate the suppression of HBV replication.

Acknowledgements

The study was supported by grants from the 2007 Research Fellowship Program Award of the Japanese Society of Gastroenterology, Japan; Cathay General Hospital Medical Center, Taiwan; and the National Taiwan University Hospital, Taiwan.

Part of this study had been presented at the *43rd Annual Meeting of the European Association for the Study of the Liver (EASL)* on 23–27 April 2008 in Milan, Italy [23] and won the Young Investigators' Full Bursaries.

The authors thank Yoshiko Nakata, Rie Akiyama, Sachi Tanaka, Miyuki Matsushita and Huei-Ling You for their technical assistance.

Disclosure statement

The authors declare no competing interests.

References

1. Lee WM. Hepatitis B virus infection. *N Engl J Med* 1997; 337:1733–1745.
2. Kao JH, Chen DS. Overview of hepatitis B and C viruses. In Goedert JJ (Editor). *Infectious Causes of Cancer: Targets for Intervention.* Totowa: Humana Press 2000; pp. 313–330.
3. McQuilland GM, Townsend TR, Fields HA, Carrol M, Leahy M, Polk BF. Seroepidemiology of hepatitis B virus infection in the United States 1976 to 1980. *Am J Med* 1989; 87 Suppl 1:S5–S10.
4. Chen DS. From hepatitis to hepatoma: lessons from type B viral hepatitis. *Science* 1993; 262:369–370.
5. Ganem D, Varmus HE. The molecular biology of the hepatitis B viruses. *Annu Rev Biochem* 1987; 56:651–693.
6. Lok ASF, McMahon BJ. AASLD practice guidelines. Chronic hepatitis B. *Hepatology* 2007; 45:507–539.
7. Doong SL, Tsai CH, Schinazi RF, Liotta DC, Cheng YC. Inhibition of the replication of hepatitis B virus *in vitro* by 2′,3′-dideoxy-3′-thiacytidine and related analogues. *Proc Natl Acad Sci U S A* 1991; 88:8495–8499.
8. Dienstag JL. Hepatitis B virus infection. *N Engl J Med* 2008; 359:1486–1500.
9. Zhang W, Hacker HJ, Tokus M, Bock T, Schroder CH. Patterns of circulating hepatitis B virus serum nucleic acids during lamivudine therapy. *J Med Virol* 2003; 71:24–30
10. Hatakeyama T, Noguchi C, Hiraga N, *et al.* Serum HBV RNA is a predictor of early emergence of the YMDD mutant in patients treated with lamivudine. *Hepatology* 2007; 45:1179–1186.
11. Schalm SW, Heathcote J, Cianciara J, *et al.* Lamivudine and alpha interferon combination treatment of patients with chronic hepatitis B infection: a randomized trial. *Gut* 2000; 46:562–568.
12. Sarin SK, Kumar M, Kumar R, *et al.* Higher efficacy of sequential therapy with interferon-alpha and lamivudine combination compared to lamivudine monotherapy in HBeAg positive chronic hepatitis B patients. *Am J Gastroenterol* 2005; 100:2463–2471.
13. Sarin SK, Sood A, Kumar M, *et al.* Effect of lowering HBV DNA levels by initial antiviral therapy before adding immunomodulator on treatment of chronic hepatitis B. *Am J Gastroenterol* 2007; 102:96–104.
14. McClary H, Koch R, Chisari FV, Guidotti LG. Relative sensitivity of hepatitis B virus and other hepatotropic viruses to the antiviral effects of cytokines. *J Virol* 2000; 74:2255–2264.
15. Wieland SF, Guidotti LG, Chisari FV. Intrahepatic induction of alpha/beta interferon eliminates viral RNA-containing capsids in hepatitis B virus transgenic mice. *J Virol* 2000; 74:4165–4173.
16. Thomas H, Foster G, Platis D. Mechanisms of action of interferon and nucleoside analogues. *J Hepatol* 2003; 39:S93–S98.
17. Pasquetto V, Wieland SF, Uprichard SL, Tripodi M, Chisari FV. Cytokine-sensitive replication of hepatitis B virus in immortalized mouse hepatocyte cultures. *J Virol* 2002; 76:5646–5653.
18. Lengyel P. Mechanisms of interferon action: the 2′5′ A synthetase-RNase L pathway. In Gresser I (Editor). *Interferon 3.* New York: Academic Press 1981; pp. 77–99.
19. Huang YW, Chayama K, Tsuge M, *et al.* Serum HBV RNA level reflects the potency of nucleos(t)ide analogue. *Hepatol Int* 2009; 3:110.

20. Rokuhara A, Matsumoto A, Tanaka E, *et al.* Hepatitis B virus RNA is measurable in serum and can be a new marker for monitoring lamivudine therapy. *J Gastroenterol* 2006; 41:785–790.

21. Gerelsaikhan T, Tavis JE, Bruss V. Hepatitis B virus nucleocapsid envelopment does not occur without genomic DNA synthesis. *J Virol* 1996; 70:4269–4274.

22. Kock J, Theilmann L, Galle P, Schlicht HJ. Hepatitis B virus nucleic acids associated with human peripheral blood mononuclear cells do not originate from replicating virus. *Hepatology* 1996; 23:405–413.

23. Huang YW, Tsuge M, Takahashi S, *et al.* Interferon inhibits HBV RNA detected during lamivudine therapy. *J Hepatol* 2008; 48:S244.

Accepted for publication 27 September 2009

Journal of General Virology (2010), **91**, 1668–1677 DOI 10.1099/vir.0.019315-0

Practical evaluation of a mouse with chimeric human liver model for hepatitis C virus infection using an NS3-4A protease inhibitor

Naohiro Kamiya,[1] Eiji Iwao,[1] Nobuhiko Hiraga,[2,3] Masataka Tsuge,[2,3] Michio Imamura,[2,3] Shoichi Takahashi,[2,3] Shinji Miyoshi,[4] Chise Tateno,[3,5] Katsutoshi Yoshizato[3,5] and Kazuaki Chayama[2,3]

Correspondence
Kazuaki Chayama
chayama@hiroshima-u.ac.jp

[1]Pharmacology Department V, Mitsubishi Tanabe Pharma Corporation, Yokohama, Japan

[2]Department of Medicine and Molecular Science, Division of Frontier Medical Science, Programs for Biomedical Research, Graduate School of Biomedical Sciences, Hiroshima University, Hiroshima, Japan

[3]Liver Research Project Center, Hiroshima University, Hiroshima, Japan

[4]DMPK Department, Mitsubishi Tanabe Pharma Corporation, Kisarazu, Chiba, Japan

[5]PhoenixBio, Higashihiroshima, Japan

A small-animal model for hepatitis C virus (HCV) infection was developed using severe combined immunodeficiency (SCID) mice encoding homozygous urokinase-type plasminogen activator (uPA) transplanted with human hepatocytes. Currently, limited information is available concerning the HCV clearance rate in the SCID mouse model and the virion production rate in engrafted hepatocytes. In this study, several cohorts of $uPA^{+/+}/SCID^{+/+}$ mice with nearly half of their livers repopulated by human hepatocytes were infected with HCV genotype 1b and used to evaluate HCV dynamics by pharmacokinetic and pharmacodynamic analyses of a specific NS3-4A protease inhibitor (telaprevir). A dose-dependent reduction in serum HCV RNA was observed. At telaprevir exposure equivalent to that in clinical studies, rapid turnover of serum HCV was also observed in this mouse model and the estimated slopes of virus decline were 0.11–0.17 $\log_{10}$ h^{-1}. During the initial phase of treatment, the $\log_{10}$ reduction level of HCV RNA was dependent on the drug concentration, which was about fourfold higher in the liver than in plasma. HCV RNA levels in the liver relative to human endogenous gene expression were correlated with serum HCV RNA levels at the end of treatment for up to 10 days. A mathematical model analysis of viral kinetics suggested that 1 g of the chimeric human liver could produce at least 10^8 virions per day, and this may be comparable to HCV production in the human liver.

Received 17 December 2009
Accepted 17 February 2010

INTRODUCTION

Hepatitis C virus (HCV) is a major cause for concern worldwide. More than 3 % of the world's population is chronically infected with HCV and 3–4 million people are newly infected each year (Wasley & Alter, 2000). Chronic HCV infection is relatively mild and progresses slowly; however, about 20 % of chronic hepatitis C (CHC) carriers progress to serious end-stage liver disease (Lauer & Walker, 2001; Liang *et al.*, 2000; Poynard *et al.*, 2003). The current standard treatment for HCV infection is administration of pegylated alpha interferon (PEG-IFN) in combination with ribavirin (RBV) for 48 weeks. The overall cure rates with this intervention are 40–50 % for patients with genotype 1 and more than 75 % for patients with genotypes 2 and 3 (Fried *et al.*, 2002; Manns *et al.*, 2001). Several compounds that inhibit specific stages of the virus life cycle have been clinically evaluated (Manns *et al.*, 2007; Pereira & Jacobson, 2009). Telaprevir is a novel peptidomimetic slow- and tight-binding inhibitor of HCV NS3-4A protease, which was discovered using a structure-based drug design approach (Perni *et al.*, 2006). A rapid decline in viral RNA was observed in CHC patients treated with telaprevir (Reesink *et al.*, 2006) and an increased antiviral effect of a combination of telaprevir and PEG-IFN has been reported (Forestier *et al.*, 2007). Recent clinical trials of telaprevir in combination with PEG-IFN and RBV have indicated a promising material advance in therapy for CHC patients (Hézode *et al.*, 2009; McHutchison *et al.*, 2009). First-generation HCV-specific agents have been developed despite the lack of small-animal models for HCV infection. However, early emergence of resistant variants against novel antiviral agents is a concern. Thus, the use of two or more investigation agents is strongly recommended for

clinical studies in CHC patients (Sherman *et al.*, 2007). To ensure ethical and safe clinical trials, animal models continue to be necessary for the mechanistic evaluation of the ability of specific agents to inhibit the virus life cycle *in vivo* and to develop better therapeutic strategies, including combination regimens (Boonstra *et al.*, 2009). Several groups have developed a small-animal model for HCV infection using homozygous urokinase-type plasminogen activator (uPA)/severe combined immunodeficiency (SCID) ($uPA^{+/+}/SCID^{+/+}$) mice transplanted with human hepatocytes (Mercer *et al.*, 2001). These mice are susceptible to cell culture-grown HCV (HCVcc; Lindenbach *et al.*, 2006) and have been used to evaluate antiviral agents including IFN-α, BILN 2061 (an NS3-4A protease inhibitor) and HCV796 (an NS5B polymerase inhibitor) (Kneteman *et al.*, 2006, 2009; Vanwolleghem *et al.*, 2007). However, the HCV clearance rate in the SCID mouse model and the virion production rate in hepatocytes engrafted in the mouse liver are not fully understood. We also generated a mouse model with an almost humanized liver (Tateno *et al.*, 2004). Using this mouse model, we reported the infection of a genetically engineered hepatitis B virus (Tsuge *et al.*, 2005) and developed a reverse genetics system for HCV genotypes 1a, 1b and 2a after intrahepatic injection of *in vitro*-transcribed RNA as well as intravenous injection of HCVcc (Hiraga *et al.*, 2007; Kimura *et al.*, 2008). In this study, we demonstrated the rapid turnover of serum HCV RNA and the pharmacokinetics (PK) and pharmacodynamics (PD) of telaprevir treatment. We concluded after quantitative estimation and the use of a mathematical model that HCV production equivalent to that in the human liver is possible in engrafted hepatocytes in this mouse model.

RESULTS

Preliminary dose-finding study

At the beginning of this study, we attempted to determine an effective dose regimen for telaprevir in this mouse model. Nine mice were randomized and treated with telaprevir over three time periods (Table 1). The lifetime kinetics of serum HCV RNA and of human serum albumin (HSA) in blood are represented in Fig. 1. One mouse (A07) exhibited a rapid reduction in HSA in the blood, which indicated the instability of human hepatocyte grafts. As a rapid reduction in HSA levels was not observed in subsequent experiments, this mouse was excluded from the mean analysis. After 7 days of twice daily (BID) dosing in period 1, the mean $\log_{10}$ changes in HCV RNA from baseline ($\pm$SEM) after the 100 and 10 mg telaprevir kg^{-1} doses were -0.49 ± 0.094 and -0.53 ± 0.039, respectively, and no dose-dependent reduction was observed. During period 2, the dose frequency was changed from BID to three times daily (TID), and the time of serum sampling was also changed from 1 to 4 h after the last dose. After the 3-day treatment, the mean $\log_{10}$ changes of HCV RNA in 100 and 10 mg telaprevir kg^{-1} TID groups were -1.00 ± 0.166 and -0.28 ± 0.056, respectively, and the difference between the two groups was significant. To test the reproducibility of results, mice were treated with 10 or 100 mg telaprevir kg^{-1} TID for 10 days and then sacrificed 5 h after the administration of the last dose. The mean $\log_{10}$ changes in serum HCV RNA were -1.46 ± 0.265 and -0.27 ± 0.073 in the 100 and 10 mg kg^{-1} TID groups, respectively, and the difference between the means was significant.

Evaluation of HCV turnover in this mouse model

Because of the SCID nature of this mouse model, the virion clearance mechanism was of interest. Six mice with steady-state and high viral loads (9.7×10^5–1.2×10^8 copies ml^{-1}) were administered 200 mg telaprevir kg^{-1} TID for 4 days, with 5 h intervals between doses and a 14 h intermission from drug treatment each day. Because the $\log_{10}$ reduction in HCV RNA appeared to depend on the time of serum collection during the day (Fig. 2a), the mean $\log_{10}$ changes in HCV RNA were plotted against time and fitted to a linear regression model (Fig. 2b). The estimated slopes (i.e. $\log_{10}$ HCV reduction per hour) and 95% confidence intervals (CI) on days 1, 2 and 3 were -0.165 (-0.268 to 0.0616), -0.115 (-0.131 to 0.0990) and -0.153, respectively. These regression lines also suggested that extrapolated HCV loads at the actual times of the daily first doses were 0.0530, -0.220 and -0.0948 $\log_{10}$ copies ml^{-1}, respectively. Therefore, it appeared that the viral load

Table 1. Telaprevir dose-finding experiment

Period	Duration (days)	Frequency of dose (per day)	Dose (mg kg^{-1})	No. of mice	Mean $\log_{10}$ changes $\pm$ SEM	*P* value (*t* test)
1	7	2	100	4	-0.49 ± 0.094	0.7806
			10	3*	-0.53 ± 0.039	
			0	1	-0.47	
2	3	3	100	4*	-1.00 ± 0.166	0.0064
			10	4	-0.28 ± 0.056	
3	10	3	100	3	-1.46 ± 0.265	0.0125
			10	3	-0.27 ± 0.073	

*One mouse was excluded because of instability of human hepatocyte grafts.

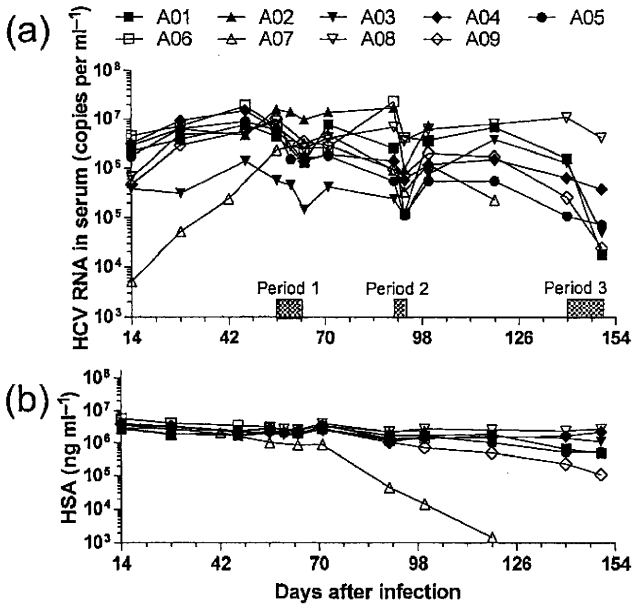

Fig. 1. Lifelong changes in serum HCV RNA and HSA in the blood of HCV-infected mice in the preliminary dose-finding experiment. Nine HCV-infected mice (A01–A09) were treated with telaprevir over three independent periods. The mice were treated with 10 mg telaprevir kg^{-1}, 100 mg telaprevir kg^{-1} or vehicle BID for 7 days (period 1), TID for 3 days (period 2) and TID for 10 days (period 3). (a) Kinetics of serum HCV RNA. (b) Kinetics of HSA level in blood. Because the HSA level indicated the stability of engrafted human hepatocytes in the mice, mouse A07 was excluded from the summary of the results in Table 1.

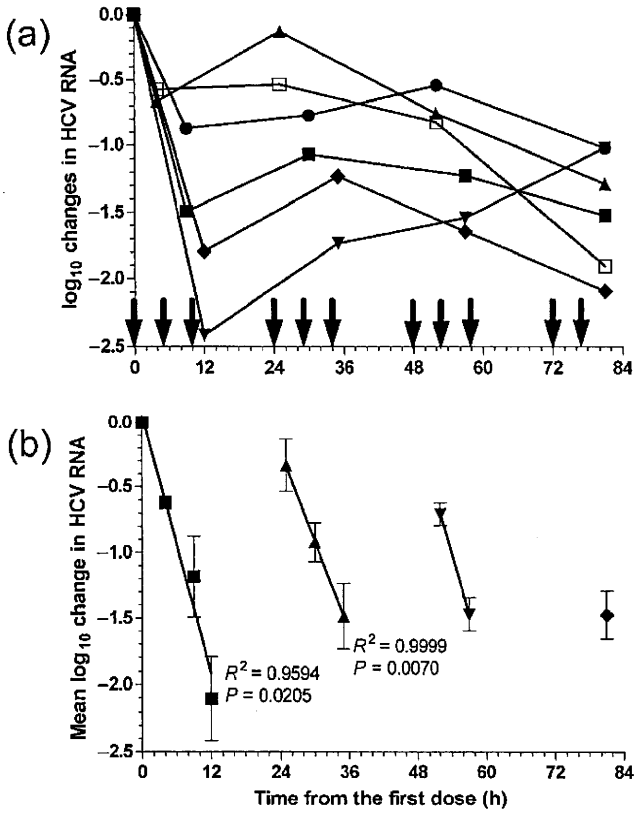

Fig. 2. Estimation of virus clearance rate. Six HCV-infected mice were treated with 200 mg telaprevir kg^{-1} TID for 4 days. Individual kinetics of log_{10} reductions in serum HCV RNA (a) and of mean log_{10} changes (±SEM) at each sampling time (b) are represented. Arrows indicate the times of dosing. The slopes of mean log_{10} HCV RNA reduction were estimated by linear regression analysis. P and R^2 values are indicated on the figure.

reverted back towards baseline levels during the 14 h intermission from drug treatment.

PK analysis

To assess drug exposure after repeated dosing in this mouse model, mice were administered 100 or 300 mg telaprevir kg^{-1} BID for 4 days. The mice receiving 300 mg kg^{-1} BID for 4 days had a mean 2 log_{10}-fold HCV reduction, whereas those receiving 100 mg kg^{-1} BID had up to a 1.5 log_{10}-fold reduction by day 3 (Fig. 3a). Plasma telaprevir concentrations after administration of the final dose are indicated in Fig. 3(b). The estimated half-life of telaprevir in the 100 and 300 mg kg^{-1} groups was 2.4 and 3.8 h, respectively.

PK/PD analysis and the dose-dependent reduction in HCV RNA

To evaluate the correlation between telaprevir concentration and HCV reductions in this mouse model, we used another cohort of 12 HCV-infected mice with high viral loads (1.6×10^6–3.9×10^8 copies ml^{-1}). In this crossover study, mice were randomized into three groups (n=4 each), each of which underwent two periods of dosing for 5 days separated by a 1-week washout period. Serum and plasma samples were collected once daily 5 h after dosing. The mean log_{10} changes in HCV RNA (±SEM) at different dose levels were calculated from the combined results of both periods (Fig. 4a). The mean log_{10} reductions from baseline in the 100 and 300 mg kg^{-1} groups were approximately 1 log_{10} and 1.5–2 log_{10}, respectively, and the difference between the two groups was statistically significant. The means calculated in each period separately are also shown in Fig. 4(b). The plasma telaprevir concentration was positively correlated with the log_{10} HCV RNA reduction level in each period (Fig. 4c).

Drug concentrations and HCV levels in blood correlate with those in the liver

The correlation between telaprevir concentrations in the plasma and liver was analysed in a double logarithmic plot 5 (dose-finding cohort) or 8 h (PK and PK/PD cohorts) after the last dose (Fig. 5). The linear regression lines suggested that telaprevir concentrations in the liver were 5–

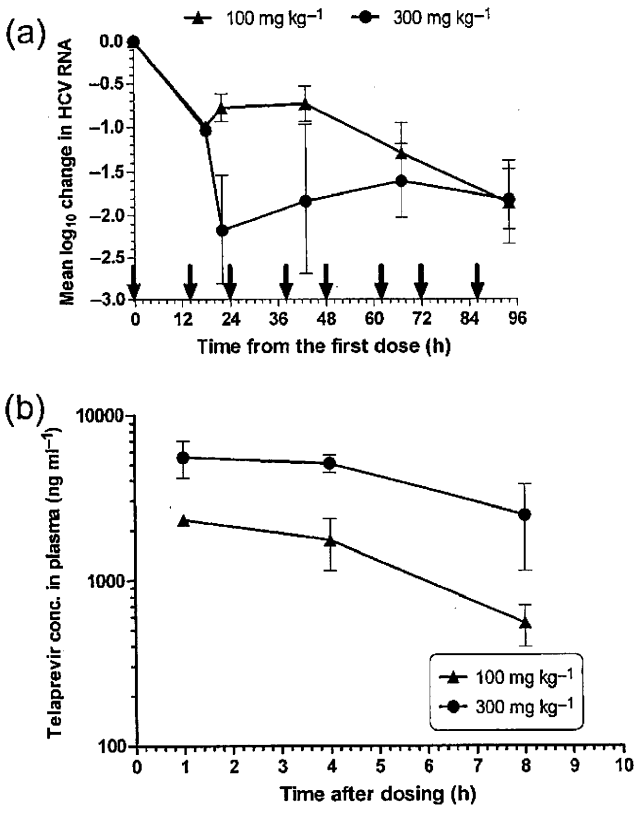

Fig. 3. PK analysis of telaprevir in the HCV-infected mouse model. Six HCV-infected mice were administered 100 (n=3) or 300 (n=3) mg telaprevir kg^{-1} BID for 4 days and serum samples were collected once daily to assess antiviral activity. After the last dose, plasma samples were collected at 1, 4 and 8 h for PK analysis. (a) Mean $\log_{10}$ changes (± SEM) in serum HCV RNA from mice treated with telaprevir. Arrows indicate the times of dosing. (b) Kinetics of telaprevir concentrations in plasma after the last dose.

10-fold higher at 5 h and approximately fourfold higher at 8 h than those in plasma. Total cellular RNA samples were extracted from two, one and four discrete small sections (approx. 50 mg) of the liver in the preliminary dose-finding, PK and PK/PD cohorts, respectively. HCV RNA levels in the total cellular RNA extract were relatively quantified by duplex real-time RT-PCR analysis using human β_2-microglobulin (hβ_2m) as an internal standard of human endogenous gene expression. Neither the threshold cycle (Ct) of hβ_2m ($Ct_{h\beta 2m}$) nor the Ct of HCV (Ct_{HCV}) correlated with total RNA from a small section of the chimeric human livers (data not shown). This result indicated that occupancy rates of human cells varied individually and/or among small sections of the chimeric human liver. Therefore, the mean difference in Ct ($\Delta Ct = Ct_{HCV} - Ct_{h\beta 2m}$) in each mouse was calculated and plotted against the viral load in serum (Fig. 6). After treatment with telaprevir for up to 10 days, mean ΔCt values ranged between 11 (HCV RNA content: $2^{11} = 2 \times 10^3$-fold lower than hβ_2m expression) and 17 (1×10^5-fold lower) among the HCV-infected mice and correlated linearly with $\log_{10}$ serum HCV RNA levels.

Viral dynamics model analysis

To evaluate time-dependent reductions in HCV with BID dosing, 12 HCV-infected elderly mice, which maintained high and steady-state viral loads (1.2×10^6–8.5×10^7 copies ml^{-1}) for more than 6 months, were treated with 200 mg telaprevir kg^{-1} BID for 3 days. The mice were divided into two groups, and serum samples were collected just before the second dose and 4 (n=6) or 8 (n=6) h after every two administrations. The single administration of telaprevir resulted in a mean 0.8–1.0 $\log_{10}$-fold reduction in HCV RNA in both groups. After the second dose, the pattern of viral kinetics appeared to depend on the time of serum collection, and the mean HCV RNA reduction level was higher in the 8 h group than in the 4 h group and plateaued at approximately a 2 $\log_{10}$-fold reduction in both groups after treatment for 3 days (Fig. 7). Finally, we attempted to estimate parameters of efficacy (ε) and virus clearance (c) per hour in this mouse model for comparison with estimates derived from human studies. Because the mean viral kinetics of the 8 h group was biphasic, the values in the 8 h group were used together for the mathematical model analysis. The estimated ε and c values were 0.992 (95 % CI 0.982–1.00) and 0.200 (95 % CI 0.110–0.291), respectively.

DISCUSSION

Using a mouse model with a chimeric human liver for HCV infection, we analysed the PK/PD of telaprevir treatment and investigated HCV dynamics during the initial phase of protease inhibitor treatment. All the mice in this study were expected to have more than half of their livers repopulated by human hepatocytes (Tateno *et al.*, 2004), which simulates a human drug metabolism profile (Katoh *et al.*, 2007, 2008). After the infection with HCV genotype 1b, high viral loads were maintained in the mice for more than 6 months. Recent studies have indicated the utility of a human/mouse chimera model for HCV infection to evaluate antiviral efficacy (Kneteman *et al.*, 2006, 2009) and preclinical safety (Vanwolleghem *et al.*, 2007). However, PK/PD studies and estimations of virus clearance rate have rarely been performed in this mouse model. HCV production, including intracellular replication in engrafted hepatocytes, has also not yet been elucidated. Despite the SCID nature of this mouse model, a 2 $\log_{10}$-fold HCV RNA reduction was observed within 0.5 days, as has been observed previously in CHC patients (Forestier *et al.*, 2007; Reesink *et al.*, 2006). In this mouse model, the rapid rebound in HCV load during the intermission from drug exposure indicated the rapid production and release of HCV into the circulation. This finding indicates that a virion-clearing compartment, which does not depend on T- and B-cell responses, may exist in this mouse model.

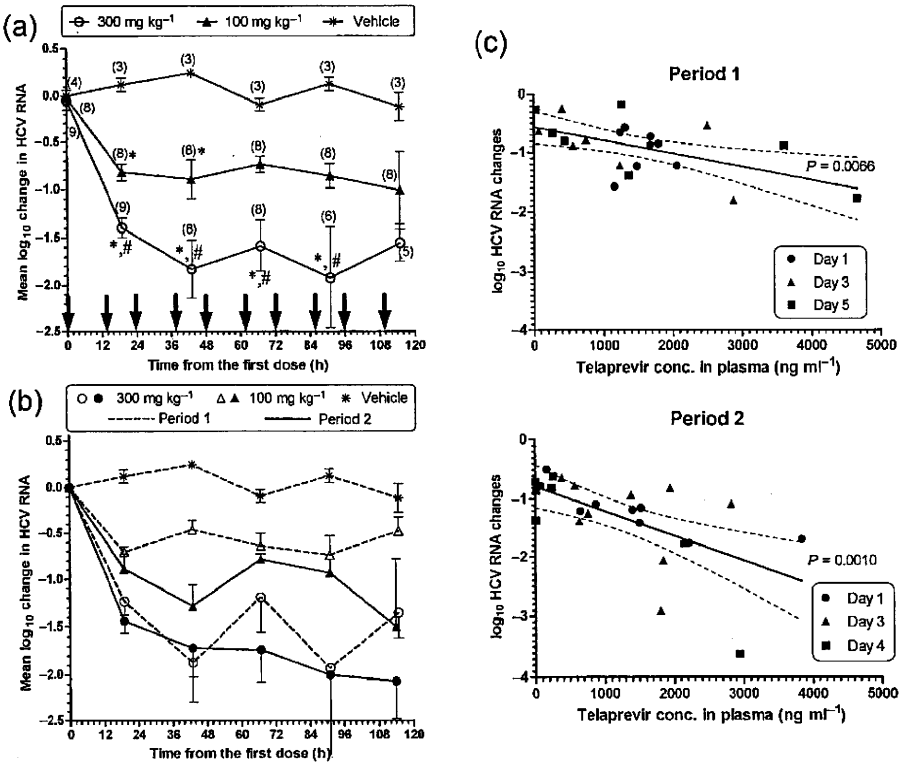

Fig. 4. PK/PD analysis and the dose-dependent reduction in HCV. Twelve HCV-infected mice were randomized into three groups (n=4 each) and then underwent two periods of telaprevir BID dosing for 5 days, separated by a 1-week washout period. Before the second period, the mice in the vehicle control group were additionally assigned to active drug groups. During the second period, mice that received the high or low doses were crossed over to the alternative treatment. Serum and plasma samples were collected once daily 5 h after dosing. Mean $\log_{10}$ changes (± SEM) in serum HCV RNA were calculated from the combined results from both periods (a) and each period separately (b). Arrows indicate the times of dosing. *, $P<0.05$ versus vehicle control group; #, $P<0.05$ versus 100 mg kg^{-1} group. (c) Correlation between $\log_{10}$ reduction in serum HCV and telaprevir concentrations in plasma. Linear regressions (solid lines) and 95% CI (dashed lines) are indicated.

One possible explanation is that viral kinetics after liver transplantation in humans may play a role in HCV clearance under immunosuppressed conditions (Dahari *et al.*, 2005; Powers *et al.*, 2006; Schiano *et al.*, 2005). This observation suggests that this mouse model is capable of evaluating 'first-phase' HCV clearance after drug treatment.

In a clinical trial of telaprevir, CHC patients who exhibited a continuous decline in viral kinetics had mean plasma trough levels above 1000 ng ml^{-1}; therefore, a dose of 750 mg TID was selected for further clinical studies (Sarrazin *et al.*, 2007). When HCV-infected mice were administered 100 or 300 mg telaprevir kg^{-1}, a plasma concentration above 1000 ng ml^{-1} was maintained beyond 8 h in mice treated with 300 mg kg^{-1} but not in those treated with 100 mg kg^{-1}. This result suggests that the extrapolation of telaprevir doses from this mouse model to human studies depends on body surface area, i.e. approximately 15th of a dose in this mouse model may be equivalent to a dose in humans. In another cohort of mice treated with 100 and 300 mg telaprevir kg^{-1} BID, a dose-dependent reduction in HCV was observed and the plasma telaprevir concentration correlated significantly with the HCV reduction level. Therefore, the PK/PD results in this mouse model may be able to indicate a targeted dose range in clinical studies.

Whereas a telaprevir concentration in plasma equivalent to its dosage in clinical trials was achieved in this mouse model, the serum HCV RNA level plateaued at a decrease of approximately 2 $\log_{10}$-fold within several days of treatment. A saturated reduction of approximately 2 $\log_{10}$-fold after treatments with BILN 2061 and IFN was also reported in an analogous mouse model (Kneteman *et al.*, 2006; Vanwolleghem *et al.*, 2007). These observations led us to examine HCV replication in the chimeric human liver. In the relative quantification of HCV RNA against human-specific endogenous gene expression, we observed a correlation between the serum HCV RNA level and the mean ΔCt value in the liver, despite no correlation between the total RNA concentration and each Ct value of two target genes in the liver RNA extracts. This result can be interpreted to indicate that HCV replicated only in

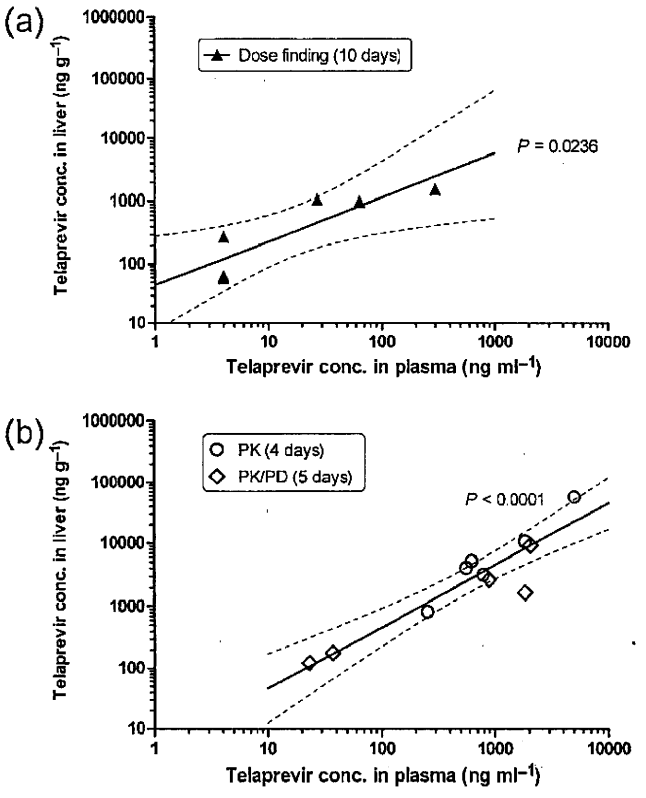

Fig. 5. Correlation between telaprevir concentrations in the liver and plasma. Telaprevir concentrations in the liver and plasma were determined at the end of the three different experiments indicated in Fig. 1 (dose-finding), Fig. 3 (PK) and Fig. 4 (PK/PD). Telaprevir concentrations in the liver were plotted against those in plasma 5 (a) or 8 (b) h after the last dose. Linear regressions (solid lines) and 95 % CI (dashed lines) are indicated.

engrafted human hepatocytes, and the observed HCV reduction in serum might reflect virus replication in the human hepatocyte grafts. Moreover, the relative content of HCV RNA was 2×10^3–1×10^5-fold lower than hβ_2m expression, whereas an HCV replicon cell line, which had approximately 1000 replicon genomes per cell (Quinkert *et al.*, 2005), contained nearly equal amounts of both genes (data not shown). HCV replication was much lower in the engrafted human hepatocytes than in an HCV replicon cell line, and HCV infected only a small portion of the engrafted human hepatocytes. It has been reported that 4–25 % of hepatocytes in a CHC patient were positive for replicative-intermediate RNA, and the mean number of viral genomes per productively infected hepatocyte ranged from 7 to 64 molecules (Chang *et al.*, 2003). Also, a more recent report suggested that the percentage of HCV antigen-positive hepatocytes in patients varied from 0 to 40 %, and the HCV content in 2000 microdissected HCV-positive cells ranged from 40 to 1800 international units using a branched DNA assay (Vona *et al.*, 2004). Therefore, we suggest that HCV replication efficiency in engrafted human hepatocytes is equivalent to that in CHC patients.

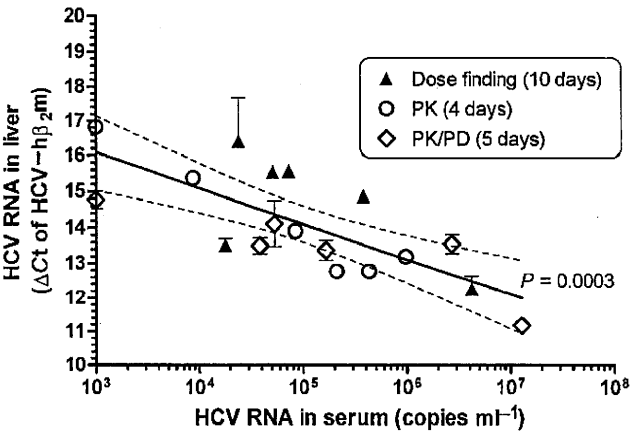

Fig. 6. Correlation between HCV content in the liver and serum. Relative quantification of HCV RNA levels in the liver was determined by the difference between threshold cycles (ΔCt) of HCV RNA and hβ_2m in a duplex real-time RT-PCR analysis. Linear regressions (solid line) and 95 % CI (dashed lines) are indicated.

The differences observed between the engrafted human hepatocytes and the HCV replicon cell line can be explained by the following assumptions: approximately 10 % of engrafted human hepatocytes are productively

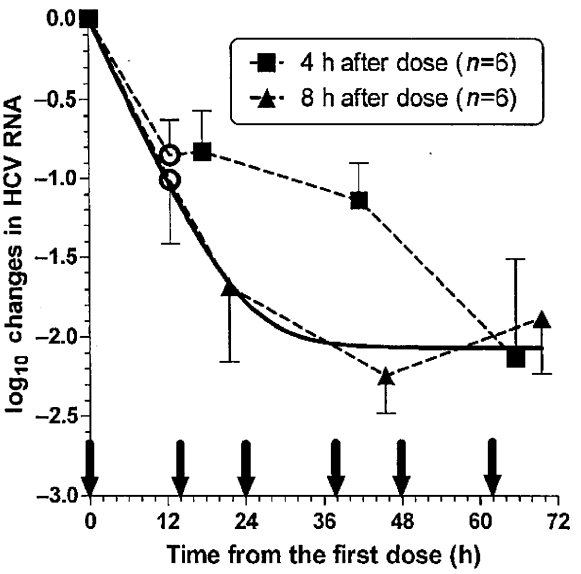

Fig. 7. Viral dynamics under BID telaprevir treatment. Mice were administered 200 mg telaprevir kg^{-1} BID at the times indicated by arrows. Serum samples were collected just before the second dose was administered and 4 (n=6) or 8 (n=6) h after every two doses were administered. Mean $\log_{10}$ changes (±SEM) in serum HCV RNA are plotted. The solved equation described in Methods was fitted to the values in the 8 h group (solid line), and the estimated efficacy and virion clearance rates were 0.992 (95 % CI 0.982–1.00) and 0.200 (95 % CI 0.110–0.291), respectively.

infected and harbour approximately ten HCV genomes per cell at baseline steady state and a 2 $\log_{10}$-fold reduction is achieved with drug treatment.

Mathematical models have proven valuable in understanding the *in vivo* dynamics of HCV, and very rapid dynamic processes occur on timescales of hours to days, and slower processes occur on timescales of weeks to months (Perelson & Ribeiro, 2008). In the last experiment, we observed a biphasic decline in the HCV RNA level after BID dosing for 3 days. During the first 2 days of the treatment, a discrepancy in viral kinetics between the serum-sampling time points was noted. Similarly, fluctuations in viral kinetics during the first-phase slope were observed in patients who received IFN three times a week (Pawlotsky *et al.*, 2004). Variable efficacy rate determined by PK parameters can explain fluctuations during the first-phase slope in mathematical model analysis (Talal *et al.*, 2006). However, it is difficult to evaluate the individual temporal changes in viral and drug kinetics using a mouse model as only a limited volume of blood is available for analysis. Therefore, we assumed a constant efficacy rate (ε) and omitted a turnover rate of hepatocytes because of the short duration of treatment. The estimated clearance rate (c) in this study was 4.8 day^{-1}. Additionally, the mean slope of 0.144 $\log_{10}$ h^{-1} (Fig. 2b) could be transformed to 0.332 h^{-1}=8.0 day^{-1} according to the change of base of a logarithm. The estimated clearance rates in this mouse model basically agreed with estimates determined in humans infected with HCV genotype 1 and undergoing IFN-based therapies (Herrmann *et al.*, 2003; Neumann *et al.*, 1998; Pawlotsky *et al.*, 2004) or large-volume plasma apheresis (Ramratnam *et al.*, 1999). Total virion production during steady-state viral kinetics in this mouse model was calculated by multiplying c by the initial viral load (V_0) and then normalizing the extracellular fluid volume. From previous studies, it was determined that 10^{11}–10^{13} virions are produced daily in patients with high HCV loads (Neumann *et al.*, 1998; Ramratnam *et al.*, 1999). In this mouse model, the volume of extracellular fluid and weight of the liver were approximately 20 and 9 % of the body weight (data not shown), and the mean $\log_{10}$ V_0 ($\pm$SEM) among the mice with mean clearance rates of 4.8 and 8.0 per day were 6.96 ± 0.26 and 7.00 ± 0.33, respectively. The results of the calculations indicated that 1 g of the chimeric human liver produced 1×10^8–2×10^8 virions per day. The typical weight of the human liver is 1–2 kg; thus, the capacity of human hepatocytes to produce HCV in this mouse model may be equivalent to that in CHC patients. In conclusion, a mouse model with a chimeric human liver can simulate HCV replication in human patients quantitatively and dynamically, and this mouse model may be suitable for preclinical evaluations of novel HCV-specific agents and other therapeutic strategies, including combination regimens.

METHODS

Generation of mice with chimeric human livers and HCV infection. The generation of uPA$^{+/+}$/SCID$^{+/+}$ mice and transplantation of frozen human hepatocytes was performed at PhoenixBio. Graft function was monitored on the basis of HSA levels in blood (Tsuge *et al.*, 2005). All the mice had high HSA levels, which suggested that nearly half of their livers were repopulated by human hepatocytes (Tateno *et al.*, 2004). After obtaining written informed consent, we collected sera periodically from patients who were chronically infected with HCV genotype 1b and failed to respond to PEG-IFN and RBV therapy. The mice were inoculated with the serum samples via the orbital vein after anaesthetization. The experimental protocol was approved by the Ethics Review Committee for Animal Experimentation of the Graduate School of Biomedical Sciences, Hiroshima University.

Compound preparation and experimental designs. The telaprevir formulations were kindly provided by Vertex Pharmaceuticals. A telaprevir suspension was prepared as described previously (Perni *et al.*, 2006) and used in experiments 1 and 2. In the other experiments, a telaprevir suspension was prepared daily as in the tablet formulation (Forestier *et al.*, 2007; Hézode *et al.*, 2009; McHutchison *et al.*, 2009). A suspension of telaprevir was administered via oral gavage.

Experiment 1: preliminary dose-finding study. Ten out of 11 mice developed serum HCV loads greater than 10^4 copies ml^{-1}. Nine mice with high viral loads (>10^5 copies ml^{-1}) were randomized and administered 10 or 100 mg telaprevir kg^{-1} BID or TID over three periods. During period 1, the mice were administered 100 (n=4) or 10 (n=4) mg telaprevir kg^{-1} or vehicle (n=1) BID at 18:00 and 10:00 h for 7 days, and serum samples were collected before treatment and 1 h after administration in the morning on the third and/or seventh day. During period 2, the mice were administered 100 (n=5) or 10 (n=4) mg telaprevir kg^{-1} TID for 3 days, and serum samples were collected before treatment and 4 h after administration of the last dose. Three mice died between periods 2 and 3. During period 3, the mice were administered 100 (n=3) or 10 (n=3) mg telaprevir kg^{-1} TID for 10 days. The mice were sacrificed 5 h after administration of the last dose, and plasma, serum and liver samples were collected.

Experiment 2: evaluation of HCV turnover. Eleven mice were infected with HCV and eight mice survived for more than 15 weeks with steady-state and high viral loads (10^6–10^8 copies ml^{-1}). Six of the mice were administered 200 mg telaprevir kg^{-1} TID at 9:00, 14:00 and 19:00 h for 4 days. On day 1, serum samples were collected before dose administration, 4 h after the first and second doses were administered, and 2 h after the third dose was administered (n=2 each). On day 2, serum samples were collected 1 h after each of the three doses was administered (n=2 each). Serum samples were also collected 4 h after the first and second doses were administered on day 3 (n=3 each) and 4 h after the second dose was administered on day 4.

Experiment 3: PK analysis. After a washout period, six mice from experiment 2 were administered 100 or 300 mg telaprevir kg^{-1} (n=3 each) BID at 19:00 and 9:00 h for 4 days. Serum samples were collected before dose administration, 4 (n=1) or 8 (n=2) h after administration of the second dose, and 5 h after every two doses were administered. After the final dose was administered, plasma for PK analysis was collected at 1 and 4 h. The mice were sacrificed at 8 h, and serum, plasma and liver samples were collected.

Experiment 4: dose dependence and PK/PD analysis. Thirty-six mice were infected with HCV and 13 survived for more than 13 weeks. The median survival time of this cohort was 81 days after infection. Twelve HCV-infected mice were randomized into three groups (A–C; n=4 each) and underwent two periods of BID dosing for 5 days, which were separated by 1-week washout periods. During the first period, the mice in groups A, B and C were administered 300 mg telaprevir kg^{-1}, 100 mg telaprevir kg^{-1} and vehicle,

respectively. Because two mice in group A and two mice in group C died before the second period, two remaining mice in group C and one back-up mouse were assigned to group A (n=2) and group B (n=1). During the second period, mice that received high or low doses were crossed over to the alternative treatment. Serum samples were collected before the first dose was administered and 5 h after every two doses were administered. Plasma samples were also collected at the same time on days 1, 3 and 5 in the first period and days 1, 3 and 4 in the second period. The mice were sacrificed 8 h after administration of the final dose, and serum, plasma and liver samples were collected.

Experiment 5: viral kinetics with BID dosing After infection of 45 mice, 12 HCV-infected mice maintained steady-state and high viral loads (1.2×10^6–8.5×10^7 copies ml^{-1}) for more than 6 months. The median survival time of this cohort was 131 days after infection. These mice were treated with 200 mg telaprevir kg^{-1} BID at 19:00 and 9:00 h for 3 days. The mice were divided into two groups and serum samples were collected just before the second dose was administered and 4 (n=6) or 8 (n=6) h after every two doses were administered.

Serum RNA extraction and HCV RNA quantification. HCV RNA was isolated from 10 µl serum under denaturing conditions using a SepaGene RV-R kit (Sanko Junyaku). The dried precipitates were dissolved in 10 µl diethylpyrocarbonate-treated water. Extracts were duplicated and assayed by quantitative real-time RT-PCR using TaqMan EZ RT-PCR core reagents (Applied Biosystems). Nucleotide positions of the probe and primer sets refer to HCV H77 strain (GenBank accession no. AF009606). The TaqMan probe 5′-6-FAM-CTGCGGAACCGGTGAGTACAC-BHQ-1-3′ (nt 148–168) was purchased from Biosearch Technologies, and the forward (5′-CGGGAGAGCCATAGTGG-3′; nt 130–146) and reverse (5′-AGTACCACAAGGCCTTTCG-3′; nt 272–290) primers were purchased from Sigma-Aldrich. The 25 µl RT-PCR mixture contained 0.2 nmol forward and reverse primers ml^{-1}, 0.3 nmol TaqMan probe ml^{-1} and 5 µl extracted RNA, and was monitored using a PRISM 7900HT sequence detection system (Applied Biosystems). The thermal profile was 2 min at 50 °C, 30 min at 60 °C for reverse transcription and 5 min at 95 °C, followed by 45 cycles of 20 s at 95 °C and 1 min at 62 °C. The HCV replicon I_{389}neo/NS3-3′/5.1 (Lohmann *et al.*, 1999) RNA was transcribed *in vitro* using a T7 RiboMax Express Large Scale RNA Production System (Promega) and purified twice using gel filtration. The concentration of this transcribed RNA was determined by absorbance at 260 nm and serially diluted 10-fold to prepare a standard curve for each assay.

Liver RNA extraction and HCV RNA quantification. A Wizard SV total RNA Isolation System (Promega) was used to obtain a DNase I-treated total RNA sample. The total RNA concentration was determined by absorbance at 260 nm. Total RNA samples were assayed by duplex real-time RT-PCR for relative quantification of HCV RNA using endogenous control gene expression of human β_2-microglobulin (hβ_2m; GenBank accession no. NM_004048), the TaqMan probe 5′-CAL Fluor Orange 560-AGTGGGATCG-AGACATGTAAGCAGCATCAT-BHQ-1-3′ (nt 401–430), and the forward and reverse primer set of 5′-TTGTCACAGCCCAA-GATAGTT-3′ (nt 379–399) and 5′-TGCGGCATCTTCAAACC-3′ (nt 434–450). To adjust the efficacy of PCR amplification of both target genes, the reaction condition was modified from the HCV single-probe assay. The temperature for extension was 60 °C, the concentration of the HCV probe was 0.24 nmol ml^{-1} and the reaction mixture contained the TaqMan probe/primer set for hβ_2m: 0.2 nmol primers ml^{-1} and 0.12 nmol TaqMan probe ml^{-1}. Because both target genes double after one cycle of PCR, a difference in Ct between HCV and hβ2m ($\Delta Ct = Ct_{HCV} - Ct_{h\beta2m}$) theoretically indicates a relative quantity of HCV RNA per control gene expression of $2^{-\Delta\Delta Ct}$.

Determination of drug concentration. Plasma and liver samples were analysed using chiral liquid chromatography followed by tandem mass spectrometry. After reconstitution, sample extracts were separated by normal-phase chromatography on a 2×250 mm Hypersil CPS-1 column (Thermo Hypersil-Keystone) with a mobile phase of heptane:acetone:methanol (82:17:1). Analyte concentrations were determined by turbo ion spray liquid chromatography/tandem mass spectrometry in the positive-ion mode. Analysis was performed at SRL or Mitsubishi Chemical Medience.

Statistical analysis. The HCV RNA level in serum was normalized by logarithmic conversion. Statistical analysis was performed with a mixed linear model using SAS (SAS Institute). Mean differences between two groups were evaluated with Student's t-test. The difference compared with vehicle control at each time point was evaluated by Dunnett's multiple comparisons test. Linear and non-linear regression analyses were performed using GraphPad Prism 5 (GraphPad Software).

Viral dynamics model analysis. The basic mathematical model for the analysis of HCV infection *in vivo*, which is a system of three ordinary differential equations for uninfected cells (T), productively infected cells (I) and free virus (V), has been reviewed elsewhere (Perelson & Ribeiro, 2008). Briefly, one of the three equations ($dV/dt = pI - cV$), where viral particles are produced at rate p per infected cell and cleared at rate c per virion, was solved. During treatment for 2–3 days, if one assumes that the number of I is approximately constant and equal to its pre-treatment value and that the viral level was at its set-point value (V_0), then $pI = cV_0$. Using this relationship in the equation $dV/dt = (1-\varepsilon)pI - cV$, where ε is the effectiveness in blocking virion production, yields $dV/dt = (1-\varepsilon)\,cV_0 - cV$, $V(0) = V_0$ with the solution $V(t) = V_0(1-\varepsilon+\varepsilon e^{-ct})$. Because the log change of viral load at time [$\log \Delta V(t)$] equals $\log V(t)/V_0$, the solved equation [$\log \Delta V(t) = \log(1-\varepsilon+\varepsilon e^{-ct})$] was fitted to the values obtained in this study via non-linear least-squares regression in order to estimate ε and c.

ACKNOWLEDGEMENTS

We thank Drs Ichimaro Yamada, Mitsubishi Tanabe Pharma Corporation, and Ann D Kwong, Gururaj Kalkeri, Susan Almquist, Steven M. Lyons and John Randle, Vertex Pharmaceuticals, for their thoughtful discussions. This work was supported in part by Grants-in-Aid for scientific research and development from the Ministry of Education, Sports, Culture and Technology and the Ministry of Health, Labour and Welfare, Japan.

REFERENCES

Boonstra, A., van der Laan, L. J. W., Vanwolleghem, T., Harry, L. A. & Janssen, H. L. A. (2009). Experimental models for hepatitis C viral infection. *Hepatology* **50**, 1646–1655.

Chang, M., Williams, O., Mittler, J., Quintanilla, A., Carithers, R. L., Jr, Perkins, J., Corey, L. & Gretch, D. R. (2003). Dynamics of hepatitis C virus replication in human liver. *Am J Pathol* **163**, 433–444.

Dahari, H., Feliu, A., Garcia-Retortillo, M., Forns, X. & Neumann, A. U. (2005). Second hepatitis C replication compartment indicated by viral dynamics during liver transplantation. *J Hepatol* **42**, 491–498.

Forestier, N., Reesink, H. W., Weegink, C. J., McNair, L., Kieffer, T. L., Chu, H.-M., Purdy, S., Jansen, P. L. M. & Zeuzem, S. (2007). Antiviral

activity of telaprevir (VX-950) and peginterferon alfa-2a in patients with hepatitis C. *Hepatology* **46**, 640–648.

Fried, M. W., Shiffman, M., Reddy, K. R., Smith, C., Marinos, G., Gonçales, F. L., Jr, Häussinger, D., Diago, M., Carosi, G. & other authors (2002). Peginterferon alfa-2a plus ribavirin for chronic hepatitis C virus infection. *N Engl J Med* **347**, 975–982.

Herrmann, E., Lee, J.-H., Marinos, G., Modi, M. & Zeuzem, S. (2003). Effect of ribavirin on hepatitis C viral kinetics in patients treated with pegylated interferon. *Hepatology* **37**, 1351–1358.

Hézode, C., Forestier, N., Dusheiko, G., Ferenci, P., Pol, S., Goeser, T., Bronowicki, M., Bourlière, J.-P., Gharakhanian, S. & other authors (2009). Telaprevir and peginterferon with or without ribavirin for chronic HCV infection. *N Engl J Med* **360**, 1839–1850.

Hiraga, N., Imamura, M., Tsuge, M., Noguchi, C., Takahashi, S., Iwao, E., Fujimoto, Y., Abe, H., Maekawa, T. & other authors (2007). Infection of human hepatocyte chimeric mouse with genetically engineered hepatitis C virus and its susceptibility to interferon. *FEBS Lett* **581**, 1983–1987.

Katoh, M., Sawada, T., Soeno, Y., Nakajima, M., Tateno, C., Yoshizato, K. & Yokoi, T. (2007). *In vivo* drug metabolism model for human cytochrome P450 enzyme using chimeric mice with humanized liver. *J Pharm Sci* **96**, 428–437.

Katoh, M., Tateno, C., Yoshizato, K. & Yokoi, T. (2008). Chimeric mice with humanized liver. *Toxicology* **246**, 9–17.

Kimura, T., Imamura, M., Hiraga, N., Hatakeyama, T., Miki, D., Noguchi, C., Mori, N., Tsuge, M., Takahashi, S. & other authors (2008). Establishment of an infectious genotype 1b hepatitis C virus clone in human hepatocyte chimeric mice. *J Gen Virol* **89**, 2108–2113.

Kneteman, N. M., Weiner, A. J., O'Connell, J., Collett, M., Gao, T., Aukerman, L., Kovelsky, R., Ni, Z.-J., Hashash, A. & other authors (2006). Anti-HCV therapies in chimeric *scid*-Alb/uPA mice parallel outcomes in human clinical application. *Hepatology* **43**, 1346–1353.

Kneteman, N. M., Howe, A. Y. M., Gao, T., Lewis, J., Pevear, D., Lund, G., Douglas, D., Mercer, D. F., Tyrrell, D. L. J. & other authors (2009). HCV796: a selective nonstructural protein 5B polymerase inhibitor with potent anti-hepatitis C virus activity *in vitro*, in mice with chimeric human livers, and in humans infected with hepatitis C virus. *Hepatology* **49**, 745–752.

Lauer, G. M. & Walker, B. D. (2001). Hepatitis C virus infection. *N Engl J Med* **345**, 41–52.

Liang, T. J., Rehermann, B., Seeff, L. B. & Hoofnagle, J. H. (2000). Pathogenesis, natural history, treatment and prevention of hepatitis C. *Ann Intern Med* **132**, 296–305.

Lindenbach, B. D., Meuleman, P., Ploss, A., Vanwolleghem, T., Syder, A. J., McKeating, J. A., Lanford, R. E., Feinstone, S. M., Major, M. E. & other authors (2006). Cell culture-grown hepatitis C virus is infectious *in vivo* and can be recultured *in vitro*. *Proc Natl Acad Sci U S A* **103**, 3805–3809.

Lohmann, V., Körner, F., Koch, J., Herian, U., Theilmann, L. & Bartenschlager, R. (1999). Replication of subgenomic hepatitis C virus RNAs in a hepatoma cell line. *Science* **285**, 110–113.

Manns, M. P., McHutchison, J. G., Gordon, S. C., Rustgi, V. K., Shiffman, M., Reindollar, R., Goodman, Z. D., Koury, K., Ling, M.-H. & other authors (2001). Peginterferon alfa-2b plus ribavirin compared with interferon alfa-2b plus ribavirin for initial treatment of chronic hepatitis C: a randomised trial. *Lancet* **358**, 958–965.

Manns, M. P., Foster, G. R., Rockstroh, J. K., Zeuzem, S., Zoulim, F. & Houghton, M. (2007). The way forward in HCV treatment – finding the right path. *Nat Rev Drug Discov* **6**, 991–1000.

McHutchison, J. G., Everson, G. T., Gordon, S. C., Jacobson, I. M., Sulkowski, M., Kauffman, R., McNair, L., Alam, J., Muir, A. J. & other authors (2009). Telaprevir with peginterferon and ribavirin for chronic HCV genotype 1 infection. *N Engl J Med* **360**, 1827–1838.

Mercer, D. F., Schiller, D. E., Elliott, J. F., Douglas, D. N., Hao, C., Rinfret, A., Addison, W. R., Fischer, K. P., Churchill, T. A. & other authors (2001). Hepatitis C virus replication in mice with chimeric human livers. *Nat Med* **7**, 927–933.

Neumann, A. U., Lam, N. P., Dahari, H., Gretch, D. R., Wiley, T. E., Layden, T. J. & Perelson, A. S. (1998). Hepatitis C viral dynamics *in vivo* and the antiviral efficacy of interferon-α therapy. *Science* **282**, 103–107.

Pawlotsky, J.-M., Dahari, H., Neumann, A. U., Hezode, C., Germanidis, G., Lonjon, I., Castera, L. & Dhumeaux, D. (2004). Antiviral action of ribavirin in chronic hepatitis C. *Gastroenterology* **126**, 703–714.

Pereira, A. A. & Jacobson, I. M. (2009). New and experimental therapies for HCV. *Nat Rev Gastroenterol Hepatol* **6**, 403–411.

Perelson, A. S. & Ribeiro, R. M. (2008). Estimating drug efficacy and viral dynamic parameters: HIV and HCV. *Stat Med* **27**, 4647–4657.

Perni, R. B., Almquist, S. J., Byrn, R. A., Chandorkar, G., Chaturvedi, P. R., Courtney, L. F., Decker, C. J., Dinehart, K., Gates, C. A. & other authors (2006). Preclinical profile of VX-950, a potent, selective, and orally bioavailable inhibitor of hepatitis C virus NS3-4A serine protease. *Antimicrob Agents Chemother* **50**, 899–909.

Powers, K. A., Ribeiro, R. M., Patel, K., Pianko, S., Nyberg, L., Pockros, P., Conrad, A. J., McHutchison, J. & Perelson, A. S. (2006). Kinetics of hepatitis C virus reinfection after liver transplantation. *Liver Transpl* **12**, 207–216.

Poynard, T., Yuen, M.-F., Ratziu, V. & Lai, C. L. (2003). Viral hepatitis C. *Lancet* **362**, 2095–2100.

Quinkert, D., Bartenschlager, R. & Lohmann, V. (2005). Quantitative analysis of the hepatitis C virus replication complex. *J Virol* **79**, 13594–13605.

Ramratnam, B., Bonhoeffer, S., Binley, J., Hurley, A., Zhang, L., Mittler, J. E., Minarkowitz, M., Moore, J. P., Perelson, A. S. & Ho, D. D. (1999). Rapid production and clearance of HIV-1 and hepatitis C virus assessed by large volume plasma apheresis. *Lancet* **354**, 1782–1785.

Reesink, H. W., Zeuzem, S., Weegink, C. J., Forestier, N., Vliet, A., van de Wetering de Rooij, J., McNair, L., Purdy, S., Kauffman, R. & other authors (2006). Rapid decline of viral RNA in hepatitis C patients treated with VX-950: a phase Ib, placebo-controlled, randomized study. *Gastroenterology* **131**, 997–1002.

Sarrazin, C., Kieffer, T. L., Bartels, D., Hanzelka, B., Möh, U., Welker, M., Wincheringer, D., Zhou, Y., Chu, H.-M. & other authors (2007). Dynamic hepatitis C virus genotypic and phenotypic changes in patients treated with the protease inhibitor telaprevir. *Gastroenterology* **132**, 1767–1777.

Schiano, T. D., Gutierrez, J. A., Walewski, J. L., Fiel, M. I., Cheng, B., Bodenheimer, H., Jr, Thung, S. N., Chung, R. T., Schwartz, M. E. & other authors (2005). Accelerated hepatitis C virus kinetics but similar survival rates in recipients of liver grafts from living versus deceased donors. *Hepatology* **42**, 1420–1428.

Sherman, K. E., Fleischer, R., Laessig, K., Murray, J., Tauber, W. & Birnkrant, D. (2007). Development of novel agents for the treatment of chronic hepatitis C infection: summary of the FDA antiviral products advisory committee recommendations. *Hepatology* **46**, 2014–2020.

Talal, A. H., Ribeiro, R. M., Powers, K. A., Grace, M., Cullen, C., Hussain, M., Markatou, M. & Perelson, A. S. (2006). Pharmacodynamics of PEG-IFN α differentiate HIV/HCV coinfected sustained virological responders from nonresponders. *Hepatology* **43**, 943–953.

Tateno, C., Yoshizane, Y., Saito, N., Kataoka, M., Utoh, R., Yamasaki, C., Tachibana, A., Soeno, Y., Asahina, K. & other authors (2004). Near completely humanized liver in mice shows human-type metabolic responses to drugs. *Am J Pathol* **165**, 901–912.

Tsuge, M., Hiraga, N., Takaishi, H., Noguchi, C., Oga, H., Imamura, M., Takahashi, S., Iwao, E., Fujimoto, Y. & other authors (2005). Infection of human hepatocyte chimeric mouse with genetically engineered hepatitis B virus. *Hepatology* **42**, 1046–1054.

Vanwolleghem, T., Meuleman, P., Libbrecht, L., Roskams, T., De Vos, R. & Leroux-Roels, G. (2007). Ultra-rapid cardiotoxicity of the hepatitis C virus protease inhibitor BILN 2061 in the urokinase-type plasminogen activator mouse. *Gastroenterology* **133**, 1144–1155.

Vona, G., Tuveri, R., Delpuech, O., Vallet, A., Canioni, D., Ballardini, G., Trabut, J. B., Le Bail, B., Nalpas, B. & other authors (2004). Intrahepatic hepatitis C virus RNA quantification in microdissected hepatocytes. *J Hepatol* **40**, 682–688.

Wasley, A. & Alter, M. J. (2000). Epidemiology of hepatitis C: geographic differences and temporal trends. *Semin Liver Dis* **20**, 1–16.